Supplementary Information

Polyacrylamide gel as a new embedding media for the enhancement of metabolite MALDI imaging

Chenyu Yang,‡[ab] Ran Wu,‡[ab] Haiqiang Liu,‡[ab] Liang Qin,[ab] Lulu Chen,[ab] Liang Qin,[ab] Hualei Xu,[ab] Hao Hu,[ab] Jinrong Li,[ab] Hua Guo,[ab] Yiyang Shi,[ab] Dongxu Jiang,[ab] Qichen Hao,[ab] Jinchao Feng,[b] Yijun Zhou,[b] Xiangyi Liu,*[c] Gaopeng Li,*[d] and Xiaodong Wang*[ab]

[a] Key Laboratory of Mass Spectrometry Imaging and Metabolomics (Minzu University of China), State Ethnic Affairs Commission, Beijing 100081, China.

[b] Centre for Imaging & Systems Biology, College of Life and Environmental Sciences, Minzu University of China, Beijing 100081, China.

[c] Department of Laboratory Medicine, Beijing Tongren Hospital, Capital Medical University, Beijing 100730, China.

[d] General Surgery Department, Shanxi Bethune Hospital, Taiyuan 030032, China.

‡C. Y., R. W., and H. L. contributed equally to this manuscript.

***Corresponding Authors:**

Xiaodong Wang − Key Laboratory of Mass Spectrometry Imaging and Metabolomics (Minzu University of China), State Ethnic Affairs Commission; Centre for Imaging & Systems Biology, College of Life and Environmental Sciences, Minzu University of China
#27 Zhongguancun South Avenue, Beijing 100081, China
Email: Xiaodong@muc.edu.cn

Gaopeng Li − General Surgery Department, Shanxi Bethune Hospital
#99 Longcheng Street, Taiyuan 030032, China
Email: malone2001@163.com

Xiangyi Liu − Department of Laboratory Medicine, Beijing Tongren Hospital, Capital Medical University
#8 Chongwenmen Inner St, Beijing 100730, China.
Email: liuxiangyi@ccmu.edu.cn

Contents

Author Contribution Statement

X. W., X. L., and G. L. conceived the ideas; C. Y., R. W., H. L., and Q. H. carried out the MALDI-MSI experiments; C. Y., R. W., and H. L. performed the MS data analysis with the help of L. Q., L. C., H. X., H. H., and J. L.; C. Y., R. W., and H. L. wrote the initial manuscript with help of H. G., Y. S., D. J., and Q. H.; J F., Y. Z., G. L., X. L., and X. W. participated in the scientific discussion and manuscript revision; X. W., X. L., and G. L. supervised the work of C. Y., R. W., H. L., L. Q., L. C., H. X., H. H., J. L., H. G., Y. S., D. J., and Q. H..

Supplementary Information--EXPERIMENTAL SECTION

Reagents and Materials. Acrylamide (AM) and bis-acrylamide (BIS) were purchased from Amersco Inc. (OH, USA). Gelatin and agarose were purchased from Sigma-Aldrich (St. Louis, MO, USA). OCT compound was purchased from Leica Biosystems (Nussloch, Germany). Two matrices of 2-Mercaptobenzothiazole (2-MBT) and Michler's ethylketone (MEK, 4,4'-bis(diethylamino)benzophenone) were purchased from Sigma-Aldrich (St. Louis, MO, USA). Ultrapure water was obtained from a Milli-Q system (Millipore USA). All other chemicals (reagent grade or suitable chemical purity) not mentioned were obtained from Merck (Darmstadt, Germany). The rat livers were obtained from 8-week-old adult male Sprague–Dawley rats (Shanghai Super-B&K Laboratory Animal Corp. Ltd., Shanghai, China). The eyeballs were obtained from Atlantic salmon (*Salmo salar*) (Sidaokou aquatic product wholesale market, Beijing, China). All tissue samples were flash-frozen by slowly immersing them in liquid nitrogen to avoid shattering. The use of animal organs for this study was approved by the Ethics Committee of the College of Life and Environmental Sciences, Minzu University of China.

Optimization of PAAG Solution Composition. The concentration of PAAG was prepared at 2%, 4%, 8%, and 12% (AM:BIS = 20:1). Rat livers were embedded in PAAG with different concentrations and then sectioned for the maintenance effect evaluation of PAAG.

Embedding Media Preparation. Four embedding media were prepared in this study, including 4% PAAG, 10% gelatin, 1% agarose, and OCT. For PAAG embedding media preparation, the 500-mL 4% PAAG (AM:BIS=20:1) stock solution was prepared as follows: 19.05 g AM and 0.95 g BIS were dissolved in ultrapure water and diluted to 500 mL at room temperature, then the stock solution should be transferred to a brown bottle for dark storage at 4 ^{o}C. The whole preparation process does not require heating. N,N,N',N'-tetramethyl ethylenediamine and ammonium persulfate were added into the PAAG solution with the final concentrations of 0.0001% and 0.2%, respectively, before being used as an embedding medium. Gelatin and agarose were prepared by pouring the solids into a 50-mL beaker and adding ultrapure water. The beakers were then heated in a standard microwave oven without boiling over, with stirring, until the solids were completely dissolved, agarose need to be cooled to about 40 ^{o}C and gelatin to about 30 ^{o}C before being used as embedding media.

Sample Preparation. Suitable containers were prepared and filled with the media at the bottom before tissues were added. The tissues were placed on the surfaces of the solidified media, and the solution was poured into the container along the wall. After the media solidified, flash-frozen was carried out. The temperatures of agarose and gelatin were strictly controlled during the entire process.

Tissue Sectioning and Matrix Coating. According to previous studies, all the samples were sectioned at the chamber temperature of -20 °C.[1, 2] All the selected fresh frozen tissue samples were sectioned into 12 μm (rat liver) and 20 μm (Atlantic salmon eyeballs) thickness slices in a Leica CM1860 cryostat (Leica Microsystems Inc., Wetzlar, Germany) After sectioning, all these tissue slices were immediately thaw-mounted on the indium tin oxide (ITO)-coated microscope glass slides purchased from Bruker Daltonics (Bremen, Germany). These tissue sections were coated with 2-MBT and MEK, respectively, by a GET-Sprayer (I) (HIT Co., Ltd, Beijing, China). 2-MBT was prepared at a concentration of 12 mg/mL in a mixed MeOH: water: formic acid (FA) (80: 20: 0.2, v/v/v) solution. MEK was prepared at a concentration of 12 mg/mL in 90:10 MeOH/water containing 1% $NH_3 \cdot H_2O$. The matrix solutions were sprayed ten cycles (5 s spray, and 45 s drying time) on the surfaces of the rat liver and Atlantic salmon eyeball tissue sections to pre-seed a thin layer of matrix. After air-drying in a vented fume hood, the matrix solutions were evenly sprayed with fifty more cycles on the same tissue sections.

MALDI-MS. All the MS analysis was performed on an Autoflex Speed MALDI time-of-flight (TOF)/TOF mass spectrometer (Bruker Daltonics, Billerica, MA, USA) equipped with a solid-state Smartbeam Nd: YAG UV laser (355 nm, Azura Laser AG). The laser impulse energy was approximately 180 mJ, and the laser repetition rate was 2000 Hz. For metabolites *in situ* detection and imaging, mass spectra were acquired over the mass range from 100 to 2000 Da in the positive ion mode and negative ion mode. Two matrices of 2-MBT and MEK were used for the *in-situ* detection and imaging of metabolites from rat livers and Atlantic salmon eyeballs. To obtain MALDI-MS profiling data, mass spectra were recorded from an accumulation of 50 laser scans, each scan was in different regions and accumulated from 500 laser shots for both positive and negative ion modes. For MALDI-MSI, 250 *μm* laser grating step sizes were used to *in-situ* detect metabolites in Atlantic salmon eyeball tissue sections, and each scan (pixel) was accumulated from 500 laser shots.

Compounds extraction and LC-MS/MS. Lipid extraction were conducted according to a previous work[3]. Briefly, 20 mg eyeball tissue was homogenized in 200 μL of water with the aid of two 5-mm stainless steel balls for 30 s x 2 at a vibration frequency of 30 Hz by Retsch MM400 mixer (Retsch GmbH, Haan, Germany). Then, 800 μL of a mixed chloroform-methanol (1:3, v/v) solvent was added, followed by another 30-s homogenization step. After homogenization, the tube was centrifuged at 4,000 x g and 4°C for 20 minutes (Beckman Coulter Allegra X-22R centrifuge Brea, CA). The supernatants were collected and mixed with 250 μL of chloroform and 100 μL of water. After vortex mixing and centrifugation at 10,600 x g for 5 min, the lower organic phase in each tube was carefully transferred to a new tube and then dried in a Savant SPD1010 speed-vacuum concentrator (Thermo Electron Corporation, Waltham, MA) and stored at -80°C until used.

Expect for lipids, other metabolites were extracted as described by Nam *et al.*[4]. One mL of methanol/water (8:2, v/v) was added to 100 mg of eyeball tissue (liquid nitrogen grinding). The mixture was extracted in an ice water bath for 15 min and centrifuged at 20,000 x g for 10 min at 4°C. Take the supernatant and stored at -80°C until used.

Structural confirmation of the most detected mass-matched compounds was conducted using a Waters ACQUITY UPLC system coupled to a Waters Synapt HDMS quadrupole-time-of-flight (Q-TOF) mass spectrometer (Beverly, MA). The dried extract residues were dissolved in 100 μL of chloroform and 8 μL were injected onto a Waters Atlantis® Atlantis C^{18} reverse phase column (150 mm × 4.6 mm, 5 *μm*) for different compounds separations. LC/MS data were collected in both positive and negative ESI modes, with respective injections. MS/MS experiments were conducted using collision-induced dissociation (CID) at 10, 20, and 40V collision energies. Waters. *MassLynx software* (version 4.1) suite were used to process UPLC-MS data.

Data Analysis. For MS profiling data analysis, the Bruker *FlexAnalysis 3.4* software was used for the preliminary mass spectral viewing and processing, The peak lists generation were derived by setting the signal-to-noise(S/N) ratio of 3. The processed MS data were uploaded to *MetaboAnalyst* for further statistical analysis, after removing matrix peak interference. The ion maps were reconstructed by *FlexImaging 4.1* software (Bruker). With the aid of three databases, LIPID MAPS (https://www.lipidmaps.org/), HMBD (https://hmdb.ca/), and METLIN (http://metlin.scripps.edu), metabolite matching were indicated on the ion signal peak lists within the allowable mass error range of ±10 ppm. Three ion adduct forms of $[M+H]^+$, $[M+Na]^+$, and $[M+K]^+$ for positive ion mode, and one ion adduct form of $[M-H]^-$ for negative ion mode, were taken into consideration for the metabolite identification.

Hematoxylin and Eosin (H&E) Staining. H&E staining was performed according to a previous study to obtain standard histological optical images[5].

Supplementary Information—FIGURES

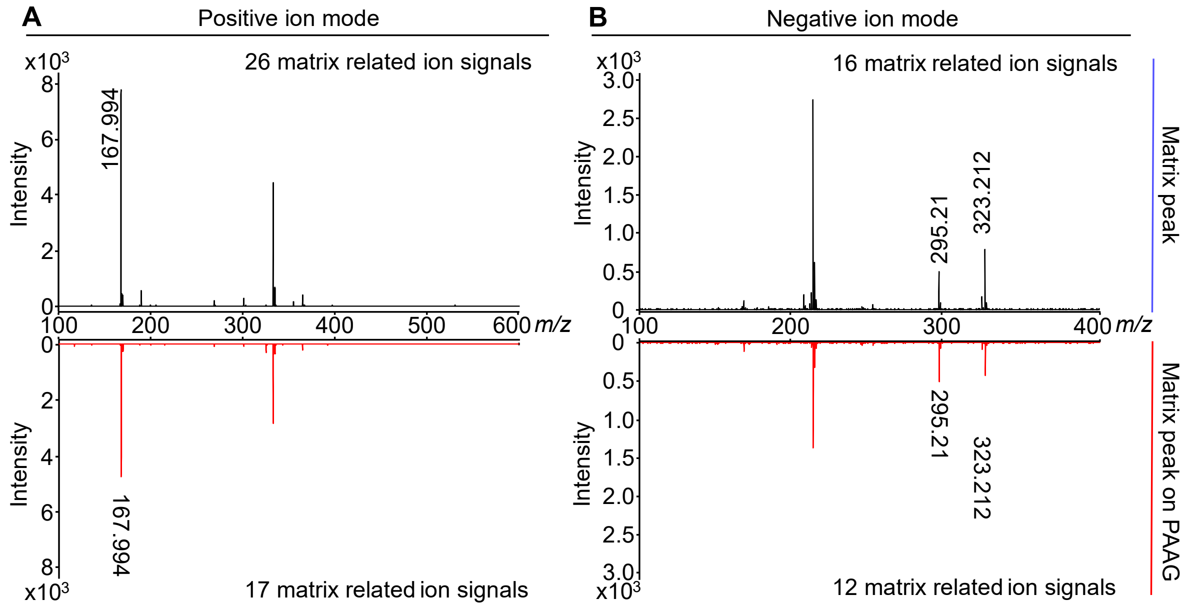

Fig. S1 Comparison of mass spectra of two matrices (2-MBT for positive ion mode, MEK for negative ion mode) with and without PAAG by (+/−)MALDI-TOF MS.

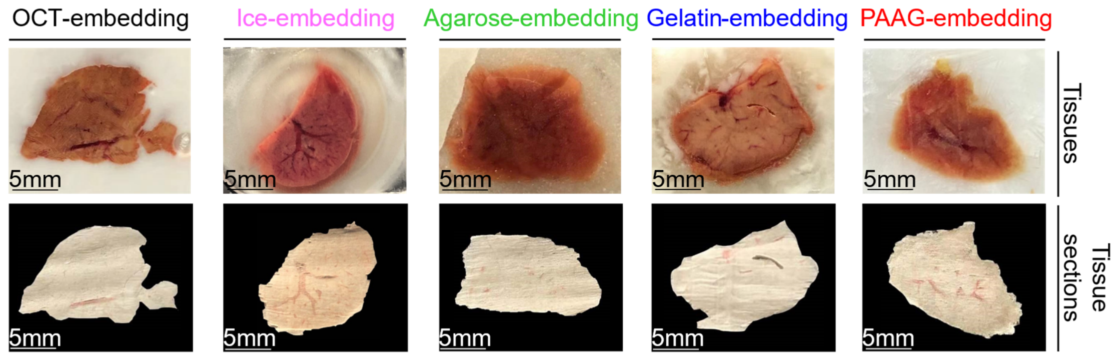

Fig. S2 Comparison of the morphological maintenance effects of five embedding media (*i.e.,* OCT, ice, agarose, gelatin, and PAAG) on rat liver tissue sectioning. The section thickness is 10 μm.

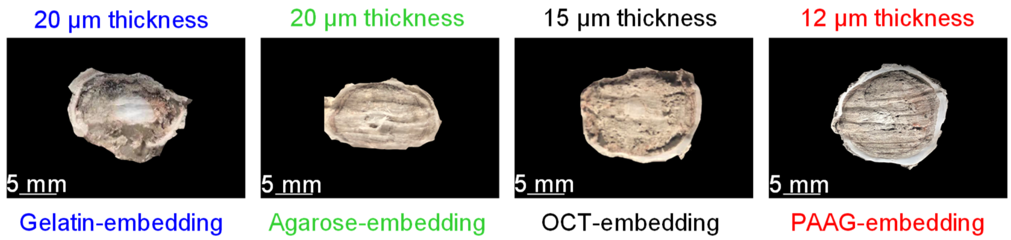

Fig. S3 Comparison of the minimum thickness of intact tissue sections of Atlantic salmon eyeballs embedded with gelatin, agarose, OCT, and PAAG, respectively.

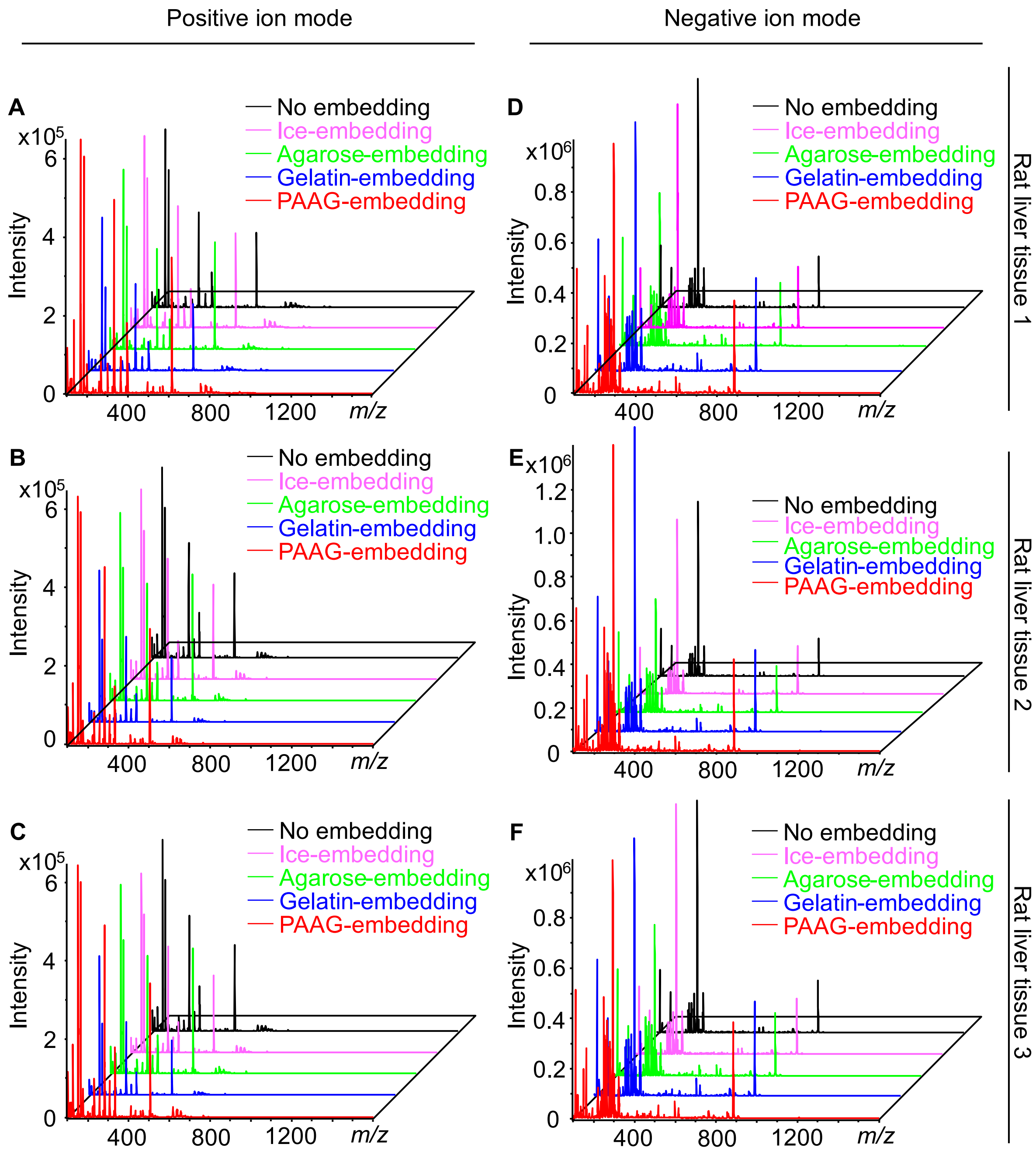

Fig. S4 Comparison of metabolites detected in rat liver tissues by MALDI-TOF MS in the positive and negative ion modes. Two compounds of 2-MBT and MEK were used as the positive and negative matrices, respectively. The targeted samples of rat liver tissues were embedded with four media, including ice, agarose, gelatin, and PAAG. (A-C) and (D-F) means the mass spectra acquired from three biological replicates.

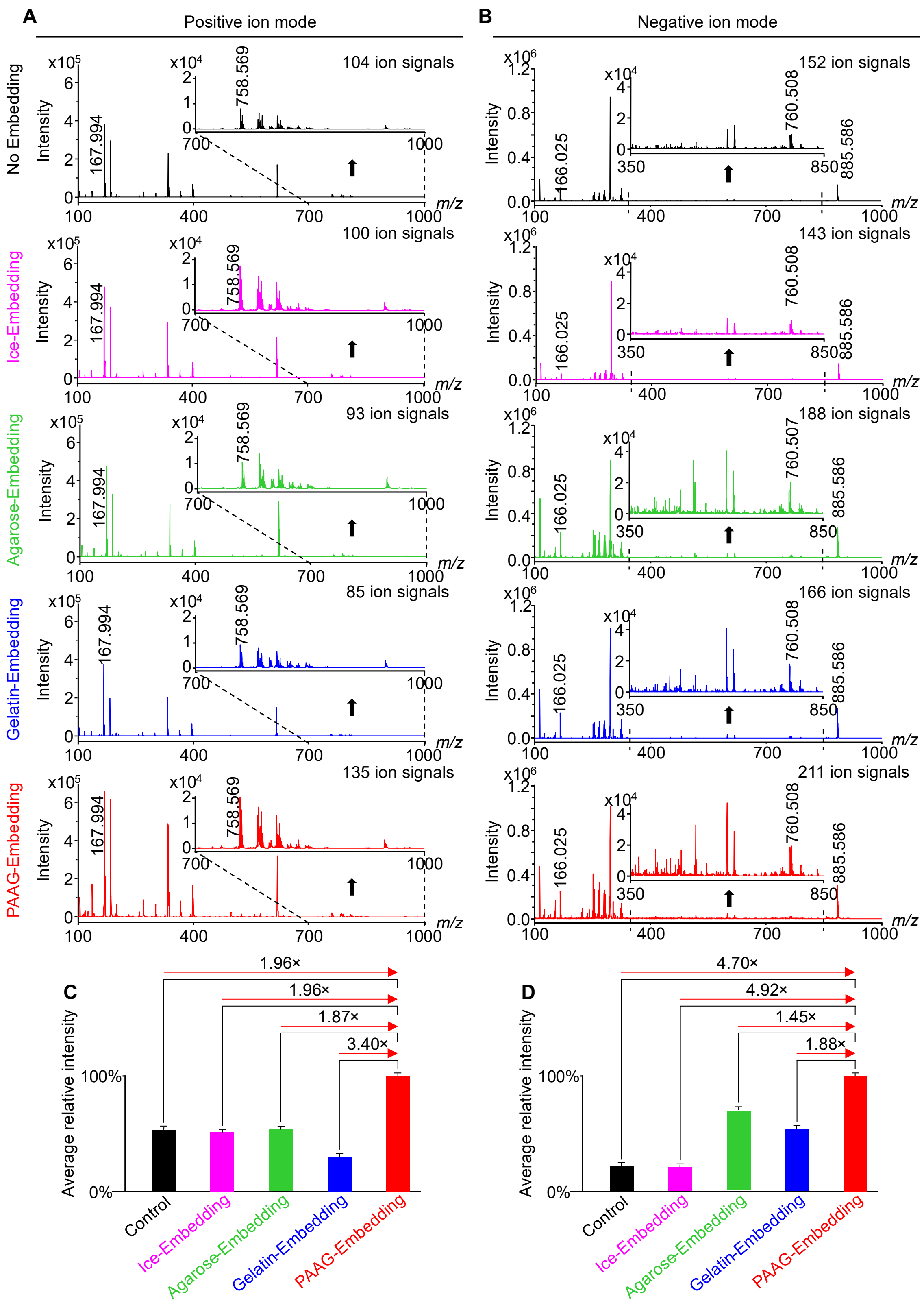

Fig. S5 Comparison of metabolites detected from rat liver tissue sections by (+/−)MALDI-TOF MS using 2-MBT and MEK as the positive and negative matrices, respectively. Before tissue sectioning, the rat liver tissues were embedded with different media, including ice, agarose, gelatin, and PAAG. One rat liver tissue without embedded medium was used as the control, the data showed in (C) and (D) were the average signal intensities statistically calculated from three biological replicates.

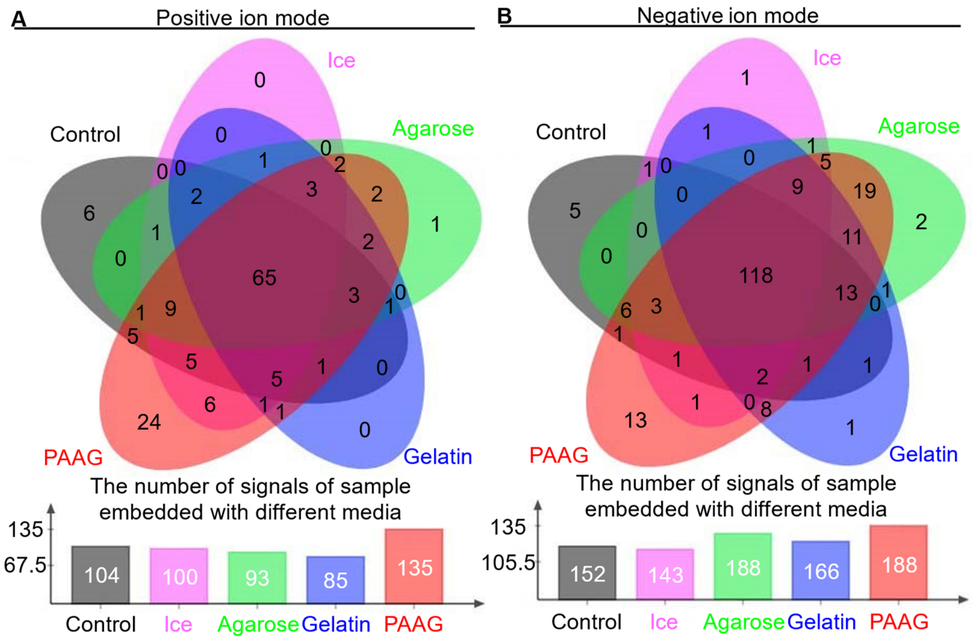

Fig. S6 Comparison of the numbers of metabolite ion signals detected in the serial tissue sections of rat liver without embedding, and embedded with ice, agarose, gelatin, and PAAG, respectively. The data showed in (A) and (B) were the average signal numbers statistically calculated from three biological replicates.

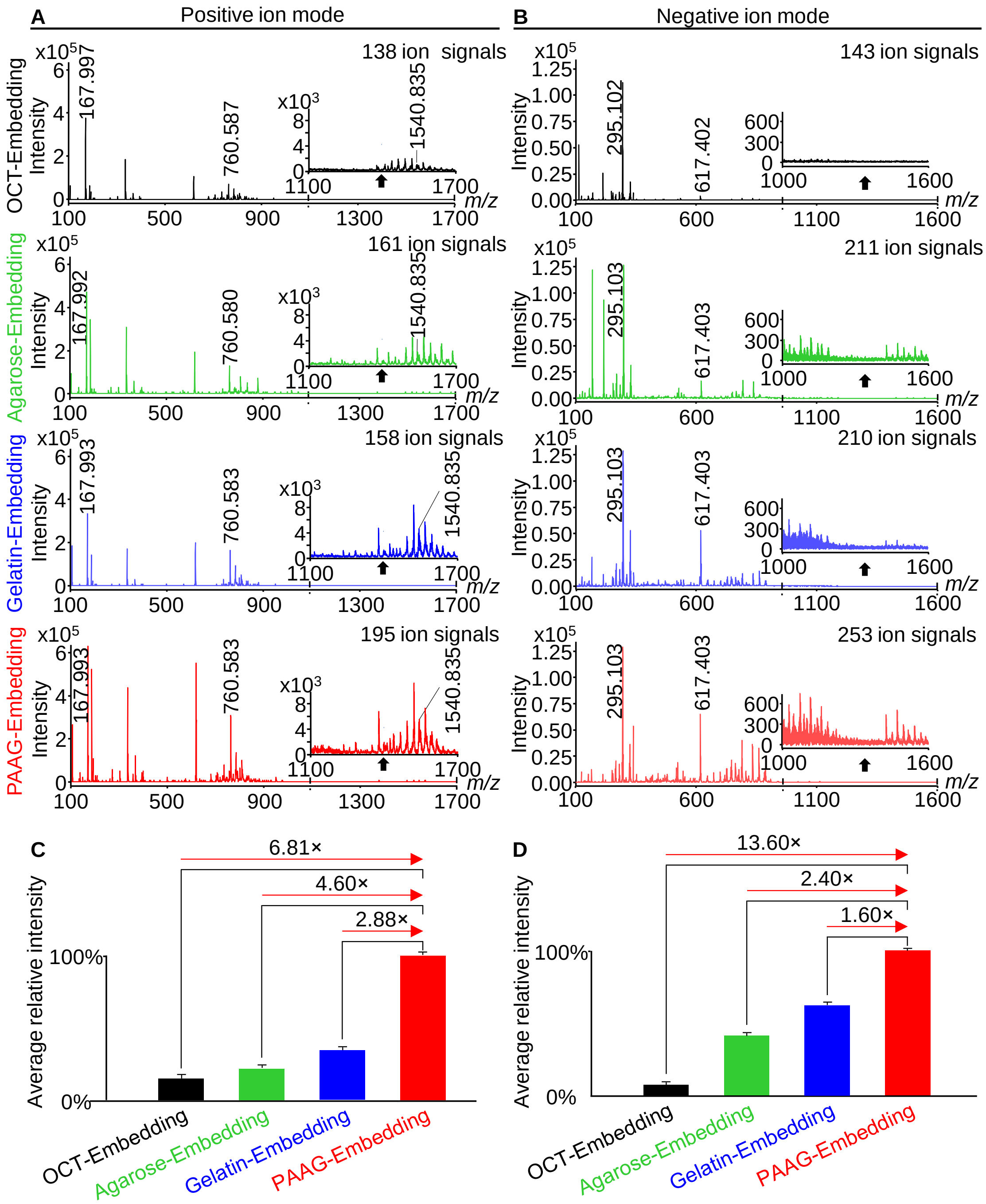

Fig. S7 (A) and (B) Comparison of metabolites detected from Atlantic salmon eyeball tissue sections *via* (+/−) MALDI-TOF MS using 2-MBT and MEK as the positive and negative matrices, respectively. Before tissue sectioning, the eyeballs were embedded with different media, including OCT, agarose, gelatin, and PAAG, respectively. (C) and (D) Data derived from (A) and (B), respectively, showing the average signal intensities statistically calculated from three biological replicates.

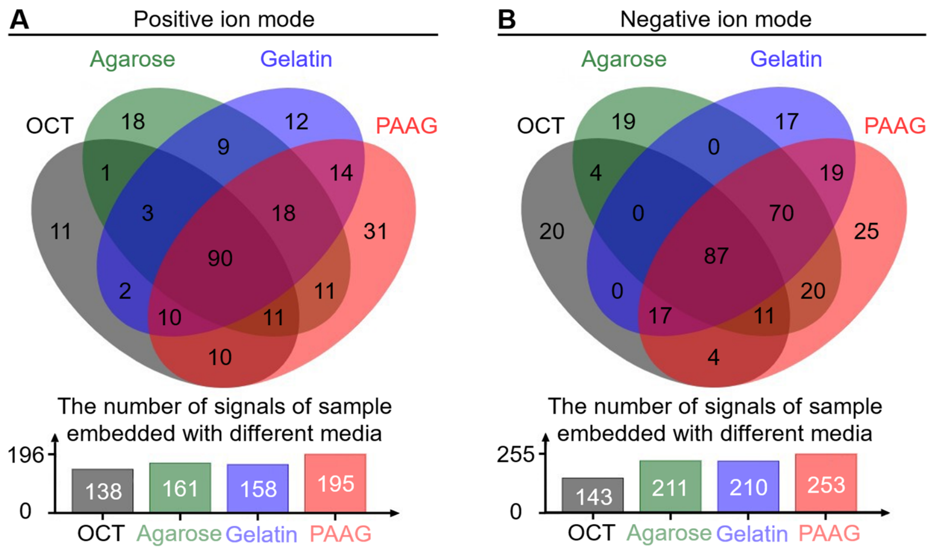

Fig. S8 Comparison of the numbers of metabolite ion signals detected in the serial tissue sections of Atlantic salmon eyeballs embedded with OCT, agarose, gelatin, and PAAG, respectively. The data showed in (A) and (B) were the average signal numbers statistically calculated from three biological replicates.

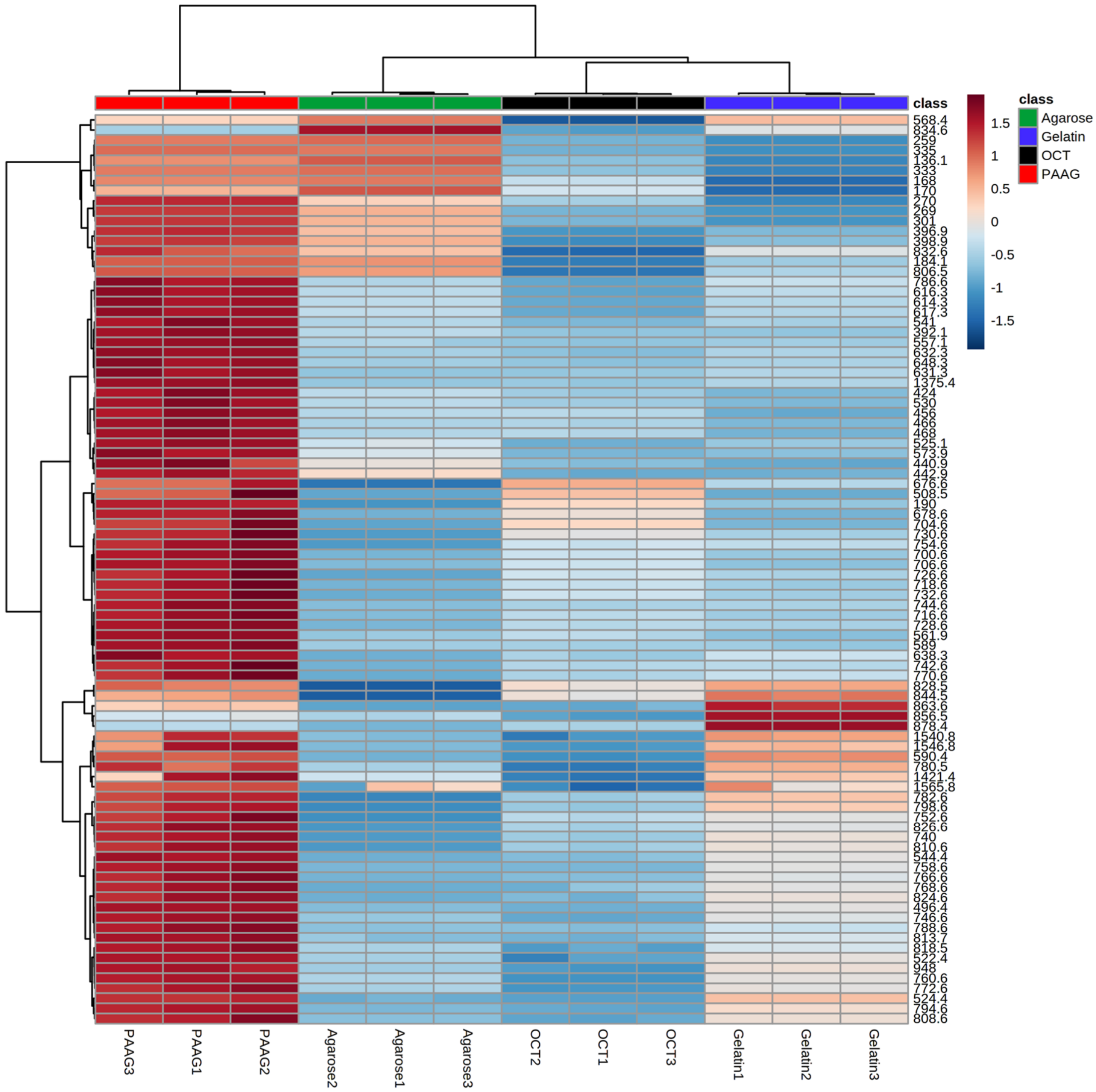

Fig. S9 The heat map of the ion signal intensities of metabolites detected in serial tissue sections of Atlantic salmon eyeballs embedded with OCT, agarose, gelatin, and PAAG media, respectively, by (+)MALDI-TOF MS using 2-MBT as the matrix (n=3×3).

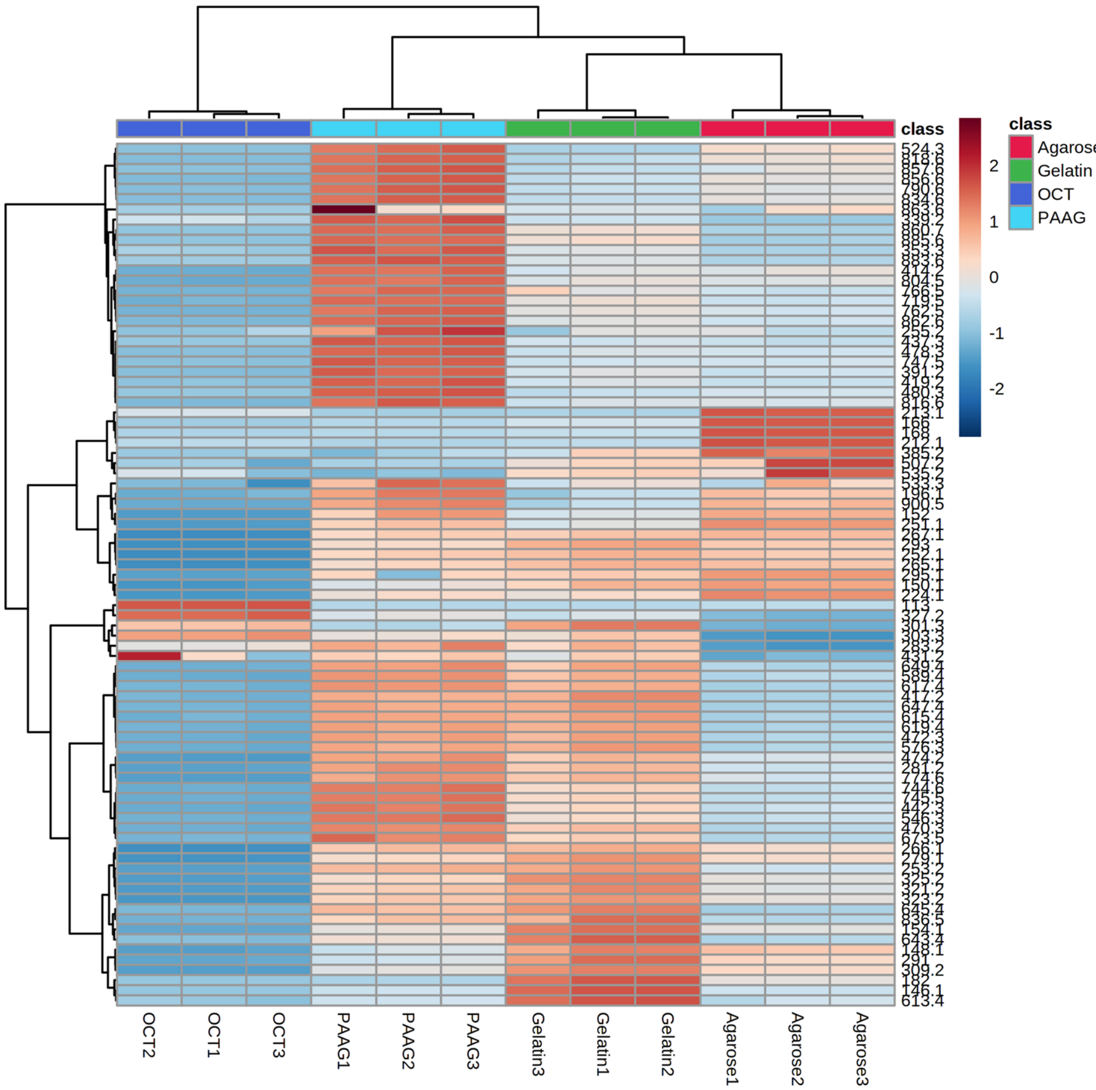

Fig. S10 The heat map of the ion signal intensities of metabolites detected in serial tissue sections of Atlantic salmon eyeballs embedded with OCT, agarose, gelatin, and PAAG media, respectively, by (-)MALDI-TOF MS using MEK as the matrix (n=3×3).

Supplementary Information--Tables

Table S1. Properties of PAAG embedding for MALDI-MSI, compared with four kinds of commonly-used media.

Embedding medium	Preparation	Physical support features	Adhesivity	Limitations	Acceptability
Ice (Pure ddH2O)	Ready to use	Hard	Poor	Not evaluated	Poor
OCT	Ready to use	Pliable	Good	PEG/PVA introduce polymer peaks into spectra, smearing causing ion suppression	Poor
1% Agarose	Fast preparation	Hard	Poor	May cause molecular degradation during heated embedding process	Acceptable
10% Gelatin	Fast preparation	Hard	Poor	May cause molecular degradation during heated embedding process	Acceptable
PAAG	Ready to use	Pliable	Good	Not observed	Good

Table S2. Comparison of metabolite ion signals detected in the tissue sections of rat liver embedded with or without ice, agarose, gelatin, and PAAG, by (+)MALDI-TOF/TOF MS using 2-MBT as the matrix (n=3×3).

Detected metabolite ion signals [a)] (*m/z*)	Rat liver tissue sections				
	Control (No embedding)	Ice-embedding	Agarose-embedding	Gelatin-embedding	PAAG-embedding
104.277	√	√	√	√	√
109.132					√
110.200					√
112.206					√
114.409	√	√	√	√	√
115.254					√
117.267					√
118.202	√	√	√	√	√
120.168					√
124.091					√
125.069	√	√	√		√
133.199					√
136.063	√	√	√	√	√
138.053					√
140.876	√	√	√	√	√
146.143		√	√	√	
147.002	√				√
156.065	√	√	√	√	√
162.109	√	√	√	√	√
162.962	√				√
166.028	√	√	√	√	√
166.943	√	√	√	√	√
167.995	√	√	√	√	√
168.997	√	√	√		√
170.000	√	√	√	√	√
170.597		√			√
181.980					√
184.056	√	√	√	√	√
189.962	√	√	√	√	√
193.989	√				√
198.062	√	√	√		√

Detected metabolite ion signals [a] (*m/z*)	Rat liver tissue sections				
	Control (No embedding)	Ice-embedding	Agarose-embedding	Gelatin-embedding	PAAG-embedding
198.925					√
199.943		√	√		√
201.937		√	√	√	√
205.952	√	√	√	√	√
222.005	√	√	√	√	√
224.051					√
224.995					√
227.019					√
229.869	√		√		√
231.874					√
241.964					√
243.966	√		√	√	√
256.982					√
258.086	√	√	√	√	√
259.013	√	√	√	√	√
268.997	√	√	√	√	√
270.006	√	√	√	√	√
271.002	√				
273.921					√
275.957	√				√
290.988	√	√	√	√	√
296.055	√	√	√	√	
300.979	√	√	√	√	√
302.986	√	√	√	√	√
325.214	√	√	√	√	√
332.963	√	√	√	√	√
334.982	√	√	√	√	√
336.968	√	√			√
364.948	√	√	√	√	√
366.944	√	√	√	√	√
390.027	√	√			√
392.047	√	√	√	√	√
396.923	√	√	√	√	√

Detected metabolite ion signals [a)] (*m/z*)	Rat liver tissue sections				
	Control (No embedding)	Ice-embedding	Agarose-embedding	Gelatin-embedding	PAAG-embedding
398.931	√	√	√	√	√
400.927	√	√	√	√	√
424.023					√
440.892	√	√	√		√
442.893	√	√	√		√
465.977		√			√
478.348					√
496.378	√	√	√	√	√
497.334	√	√	√		
498.218	√	√		√	√
499.944	√	√	√		√
513.279	√				√
520.354		√		√	√
522.376		√	√	√	√
524.406	√	√	√	√	√
529.913		√			√
534.298			√	√	√
544.243	√	√	√		√
557.216	√	√	√	√	√
572.097	√	√	√	√	√
588.999					√
614.203	√	√	√	√	√
616.225	√	√	√	√	√
630.204					√
631.207	√	√	√	√	√
632.217	√	√	√	√	√
646.173					√
648.180	√	√	√	√	√
750.145			√	√	√
751.951	√	√	√	√	√
753.911		√	√	√	√
756.511	√	√	√	√	√
758.570	√	√	√	√	√

Detected metabolite ion signals [a)] (*m/z*)	Rat liver tissue sections				
	Control (No embedding)	Ice-embedding	Agarose-embedding	Gelatin-embedding	PAAG-embedding
760.593	√	√	√	√	√
772.499	√	√	√	√	√
775.894	√	√	√	√	√
781.147	√	√	√		√
782.505	√	√		√	√
784.588	√	√	√	√	√
786.612	√	√	√	√	√
796.489	√	√	√	√	√
797.153			√		√
798.522	√	√	√	√	
799.054			√		√
800.111				√	√
804.543	√	√			√
806.577	√	√	√	√	√
808.581	√	√	√	√	√
810.614	√	√	√	√	√
812.734	√	√			√
815.130	√	√		√	√
818.511	√	√	√	√	√
820.502	√	√	√	√	√
822.520	√	√	√	√	√
824.467	√	√		√	√
828.533	√	√	√	√	√
830.535	√	√	√	√	√
831.040		√			√
832.524	√	√			√
834.579	√	√	√	√	√
838.553	√				
842.986		√	√		√
844.458	√	√	√	√	√
846.519	√	√	√	√	√
847.018		√			√
848.521	√	√		√	√

Detected metabolite ion signals [a] (*m/z*)	Rat liver tissue sections				
	Control (No embedding)	Ice-embedding	Agarose-embedding	Gelatin-embedding	PAAG-embedding
850.532	√		√	√	
851.482	√				
852.444	√			√	√
868.425	√	√	√	√	√
870.447					√
872.478	√	√	√	√	√
874.482	√				
925.463	√	√	√	√	√
946.157	√	√	√		√
948.106	√	√	√	√	√
950.116	√		√	√	√
953.510		√			√
973.474	√	√	√	√	√
980.008	√		√	√	√
1374.009			√		
1401.770	√				
1569.135	√				
Total number of detected compounds	104	100	93	85	135

a) Detected metabolite ion signal data were duplicate values obtained from three parallel detection of each group (n=3*3).

Table S3. Comparison of metabolite ion signals detected in the tissue sections of rat livers embedded with or without ice, agarose, gelatin, and PAAG, by (−)MALDI-TOF/TOF MS using MEK as the matrix (n=3×3).

Detected metabolite ion signals [a] (*m/z*)	Rat liver tissue sections				
	Control (No embedding	Ice-embedding	Agarose-embedding	Gelatin-embedding	PAAG-embedding
100.248	√	√	√	√	√
101.247	√	√	√	√	√
104.239					√
109.201					√
110.164		√	√	√	√
111.171	√	√	√	√	√
113.166	√	√	√	√	√
115.176			√		√
116.190		√	√		√
119.189	√	√	√	√	√
120.167		√	√		
121.133			√		
122.131	√	√	√	√	√
123.115	√	√	√	√	√
124.139	√	√	√	√	√
125.131		√	√	√	√
126.137	√		√		√
127.183				√	√
128.153					√
129.177					√
133.127	√	√	√		√
134.118	√	√	√	√	√
135.111	√	√	√	√	√
137.095	√	√	√	√	√
140.094	√	√	√	√	√
142.127			√	√	√
143.126			√		√
145.146		√	√		√
146.126	√		√		√
148.152	√	√	√	√	√
150.089	√	√	√	√	√
151.086	√	√	√	√	√

Detected metabolite ion signals [a] (*m/z*)	Rat liver tissue sections				
	Control (No embedding	Ice-embedding	Agarose-embedding	Gelatin-embedding	PAAG-embedding
152.068	√	√	√	√	√
153.057	√	√	√	√	√
158.062	√	√	√	√	√
159.073	√				
161.089			√	√	
163.066		√	√	√	√
164.143		√		√	
166.025	√		√	√	√
168.050	√	√		√	√
171.043			√	√	√
178.043			√		√
179.037	√	√	√	√	√
180.054	√	√	√	√	√
191.042	√				
192.118	√			√	
193.049	√				√
194.041					√
195.050			√	√	√
196.038	√	√	√	√	√
198.880					√
207.060			√		√
208.048					√
209.074				√	√
213.038			√		√
214.004	√		√	√	√
221.030		√	√		√
223.050	√	√	√	√	√
224.071	√	√	√	√	√
235.036			√		√
237.058	√	√	√	√	√
240.098			√	√	√
240.972	√	√	√	√	√
247.029			√		√
249.045		√	√	√	√

Detected metabolite ion signals [a)] (*m/z*)	Rat liver tissue sections				
	Control (No embedding	Ice-embedding	Agarose-embedding	Gelatin-embedding	PAAG-embedding
251.068	√	√	√	√	√
252.083	√	√	√	√	√
253.130		√	√		√
255.191	√	√	√	√	√
258.985	√	√	√	√	√
262.891	√	√	√	√	√
265.083	√	√	√	√	√
266.106	√	√	√	√	√
267.106	√	√	√	√	√
273.786	√	√	√	√	√
274.545		√	√	√	√
277.122			√		√
279.168	√	√	√	√	√
281.180	√	√	√	√	√
283.205	√	√	√	√	√
291.033	√	√	√	√	√
293.047	√	√	√		√
295.090		√	√	√	√
296.225	√	√	√	√	√
299.111	√	√			√
301.851					√
302.800					√
303.253	√	√	√	√	√
303.681		√			√
305.274	√	√	√	√	√
307.245	√	√	√	√	√
309.252	√	√	√	√	√
311.229			√		√
314.997		√			
315.064	√	√	√	√	√
321.209	√	√	√	√	√
322.736					√
323.212	√	√	√	√	√
323.754					√

Detected metabolite ion signals [a)] (*m/z*)	Rat liver tissue sections				
	Control (No embedding	Ice-embedding	Agarose-embedding	Gelatin-embedding	PAAG-embedding
325.239	√	√	√	√	√
327.239	√	√	√	√	√
329.261			√		√
331.275			√		√
339.200	√	√	√	√	√
349.208			√		√
353.262	√	√	√	√	√
355.070	√	√	√	√	√
362.239	√	√	√	√	√
370.201			√		√
371.203	√	√	√	√	√
384.225			√		√
386.242	√		√		√
388.256	√		√	√	√
391.234	√	√	√	√	√
399.226				√	√
409.254	√	√	√	√	√
414.268	√	√	√	√	√
417.248	√			√	√
419.264	√	√	√	√	√
428.281			√	√	√
430.194					√
433.246				√	√
435.263	√	√	√	√	√
437.258	√	√	√	√	√
442.283	√	√	√	√	√
447.274	√	√	√	√	√
452.284	√	√	√	√	√
457.229	√				
459.255	√				
462.299	√	√	√	√	√
463.266	√		√	√	√
465.298	√	√	√	√	√
470.288	√	√	√	√	√

Detected metabolite ion signals [a)] (*m/z*)	Rat liver tissue sections				
	Control (No embedding	Ice-embedding	Agarose-embedding	Gelatin-embedding	PAAG-embedding
472.283	√		√		√
473.264	√				
474.242			√		√
475.266	√	√	√	√	√
478.298	√	√	√	√	√
480.318	√	√	√	√	√
485.981			√		√
488.251	√		√		√
498.312	√		√	√	√
500.296	√	√	√	√	√
502.279	√		√	√	√
504.273	√	√	√	√	√
506.323	√	√	√	√	√
508.325	√	√	√	√	√
514.312	√	√	√	√	√
518.318	√	√	√	√	√
524.292	√	√	√	√	√
532.330	√	√	√	√	√
546.342	√	√	√	√	√
559.359			√	√	√
561.342			√		√
571.300	√	√	√	√	√
574.380			√	√	√
576.368	√	√	√	√	√
581.319	√	√	√	√	√
583.340	√	√	√	√	√
587.362	√	√	√	√	√
589.386	√	√	√	√	√
591.405			√	√	√
599.338	√	√	√	√	√
603.366		√	√	√	√
615.400	√	√	√		√
617.420	√	√	√	√	√
619.394	√	√	√	√	√

Detected metabolite ion signals [a] (*m/z*)	Rat liver tissue sections				
	Control (No embedding	Ice-embedding	Agarose-embedding	Gelatin-embedding	PAAG-embedding
642.505	√		√	√	√
645.431	√	√	√	√	√
647.432	√	√	√	√	√
656.528				√	√
671.449		√	√		√
673.482	√	√	√	√	√
687.552	√	√	√	√	√
695.442			√		√
697.477	√	√	√	√	√
699.500	√	√	√	√	√
701.519	√		√	√	√
714.505	√	√	√	√	√
716.513	√	√	√	√	√
719.463	√	√	√	√	√
721.469	√	√	√	√	√
722.518			√		
723.503	√	√	√	√	√
725.518	√	√	√	√	√
726.563	√	√	√	√	√
728.583			√	√	√
738.502	√	√	√	√	√
740.524	√	√	√	√	√
742.540	√	√	√	√	√
744.541	√		√		√
745.533	√		√	√	√
747.507	√	√	√	√	√
749.519	√	√	√	√	√
750.513			√		√
752.581			√	√	√
762.507	√	√	√	√	√
764.540	√	√	√	√	√
766.556	√	√	√	√	√
770.586	√	√	√	√	√
771.633				√	√

Detected metabolite ion signals [a)] (*m/z*)	Rat liver tissue sections				
	Control (No embedding	Ice-embedding	Agarose-embedding	Gelatin-embedding	PAAG-embedding
788.538	√	√	√	√	√
790.555	√	√	√	√	√
792.595	√		√	√	√
794.604	√		√	√	√
797.694	√		√	√	√
818.549				√	
833.554	√	√	√	√	√
835.565				√	√
857.545	√	√	√	√	√
859.570	√		√	√	√
861.585	√	√	√	√	√
871.548			√	√	√
883.525		√	√	√	√
885.586	√	√	√	√	√
887.669	√	√	√	√	√
909.639	√	√	√	√	√
911.658	√	√	√	√	√
913.671		√	√	√	√
1207.926	√	√	√	√	√
1209.922	√	√		√	√
1470.302				√	√
1472.409					√
1485.748	√	√			
Total number of detected compounds	152	143	188	166	211

a) Detected metabolite ion signal data were duplicate values obtained from three parallel detection of each group (n=3×3).

Table S4. Comparison of metabolite ion signals detected in the tissue sections of Atlantic salmon eyeballs embedded with OCT, agarose, gelatin, and PAAG, respectively, by (+)MALDI-TOF/TOF MS using 2-MBT as the matrix (n=3×3).

Detected metabolite ion signals [a)] **(m/z)**	Atlantic salmon eyeball tissue sections			
	OCT-embedding	Agarose-embedding	Gelatin-embedding	PAAG-embedding
104.345		√	√	√
105.162			√	
132.182			√	√
136.104	√	√	√	√
147.038				√
156.107				√
166.066				√
166.977	√	√		√
167.993	√	√	√	√
169.018	√	√		√
170.008	√	√	√	√
184.057	√	√	√	√
189.979	√	√	√	√
191.972				√
198.067				√
199.944				√
205.947	√		√	√
211.945				√
227.913				√
238.995				√
243.889			√	√
253.038				√
256.987				√
258.080		√		√
259.015	√	√	√	√
269.003	√	√	√	√
270.010	√	√	√	√
275.967				√
279.080				√
280.079			√	√
291.000	√	√		√
296.063			√	√

Detected metabolite ion signals [a] (*m/z*)	Atlantic salmon eyeball tissue sections			
	OCT-embedding	Agarose-embedding	Gelatin-embedding	PAAG-embedding
300.986	√	√	√	√
302.996	√	√		√
312.364				√
322.976			√	√
332.962	√	√	√	√
334.004		√		√
334.980	√	√	√	√
336.976		√		√
346.995		√		√
354.981	√	√		√
356.982			√	√
364.941				√
366.939	√			√
370.943			√	√
386.955	√		√	√
390.047		√	√	√
392.066	√	√	√	√
396.910	√	√	√	√
398.909	√	√	√	√
400.402				√
400.904				√
404.043				√
406.075				√
424.038	√	√	√	√
426.412	√			√
428.455	√			√
436.040	√			
440.913	√	√	√	√
442.889	√	√	√	√
456.026	√	√	√	√
466.022	√	√	√	√
468.013	√	√	√	√
468.420	√		√	√
478.419				√
482.415	√			√

Detected metabolite ion signals [a] (*m/z*)	Atlantic salmon eyeball tissue sections			
	OCT-embedding	Agarose-embedding	Gelatin-embedding	PAAG-embedding
494.328				√
496.375	√	√	√	√
497.992		√	√	√
499.983				√
504.435				√
508.482	√	√	√	√
515.113		√		√
518.379	√		√	√
522.396	√	√	√	√
524.408	√	√	√	√
525.117	√	√	√	√
529.960	√	√	√	√
531.924	√	√		√
534.360	√		√	√
540.991	√	√	√	√
544.380	√	√	√	√
546.366			√	
550.385		√		
557.088	√	√	√	√
558.974		√		
560.316			√	
561.911	√	√	√	√
563.868	√		√	
568.374	√	√	√	√
573.926	√	√	√	√
589.041	√	√	√	√
590.362	√	√	√	√
606.349		√	√	√
614.266	√	√	√	√
615.253		√		√
616.275	√	√	√	√
617.329	√	√	√	√
630.278		√	√	√
631.265	√	√	√	√
632.270	√	√	√	√

Detected metabolite ion signals [a] (*m/z*)	Atlantic salmon eyeball tissue sections			
	OCT-embedding	Agarose-embedding	Gelatin-embedding	PAAG-embedding
638.259	√	√	√	√
639.247	√		√	√
646.279		√		√
647.240	√			
648.260	√	√	√	√
655.066			√	√
675.524		√	√	√
676.593	√	√	√	√
678.615	√	√	√	√
683.972	√		√	√
690.525	√			
697.504		√	√	√
698.561	√		√	√
700.601	√	√	√	√
702.577			√	
704.623	√	√	√	√
706.644	√	√	√	√
711.924	√		√	√
713.498			√	
714.558	√			√
716.587	√	√	√	√
718.630	√	√	√	√
721.980		√	√	
724.576	√			√
725.569			√	
726.612	√	√	√	√
728.620	√	√	√	√
730.580	√	√	√	√
732.625	√	√	√	√
739.998	√	√	√	√
742.568	√	√	√	√
744.592	√	√	√	√
746.575	√	√	√	√
752.588	√	√	√	√
754.618	√	√	√	√

Detected metabolite ion signals [a] **(*m/z*)**	Atlantic salmon eyeball tissue sections			
	OCT-embedding	Agarose-embedding	Gelatin-embedding	PAAG-embedding
756.574		√	√	√
758.574	√	√	√	√
760.583	√	√	√	√
766.570	√	√	√	√
768.588	√	√	√	√
770.598	√	√	√	√
772.616	√	√	√	√
774.620		√	√	√
778.540	√	√	√	
780.547	√	√	√	√
782.596	√	√	√	√
786.618	√	√	√	√
788.635	√	√	√	√
792.573		√	√	√
794.608	√	√	√	√
798.582	√	√	√	√
802.569		√		
804.382		√		√
806.538	√	√	√	√
808.581	√	√	√	√
810.627	√	√	√	√
813.667	√	√	√	√
814.619		√		
818.537	√	√	√	√
820.586		√		
824.592	√	√	√	√
826.646	√	√	√	√
828.542	√	√	√	√
830.540				√
832.565	√	√	√	√
834.555	√	√	√	√
835.626	√	√		√
842.549		√		√
844.514	√	√	√	√
846.542			√	√

Detected metabolite ion signals [a] **(*m/z*)**	Atlantic salmon eyeball tissue sections			
	OCT-embedding	Agarose-embedding	Gelatin-embedding	PAAG-embedding
852.608		√		
854.568	√	√		√
856.520	√	√	√	√
863.558	√	√	√	√
870.620		√		
872.571		√	√	√
876.588		√		
878.427	√	√	√	√
900.477	√	√	√	
909.559	√			
916.631		√	√	
925.515		√	√	√
927.482		√	√	√
947.988	√	√	√	√
950.158		√		
973.418		√	√	√
993.581	√			
995.565	√			
1001.637		√		
1018.806		√	√	
1040.781		√	√	
1043.687		√		
1045.658		√	√	
1183.809		√		
1185.904		√		
1231.072		√	√	√
1255.978			√	
1279.668			√	√
1281.670			√	√
1328.272		√	√	
1347.332			√	√
1373.335	√	√		√
1375.430	√	√	√	√
1382.321	√			
1396.208		√		√

Detected metabolite ion signals [a] (*m/z*)	Atlantic salmon eyeball tissue sections			
	OCT-embedding	Agarose-embedding	Gelatin-embedding	PAAG-embedding
1402.442		√	√	√
1404.163			√	
1409.663	√			√
1421.390	√	√	√	√
1433.733				√
1435.665			√	√
1437.873	√			√
1449.931			√	
1450.450		√		
1457.688				√
1461.148	√			√
1462.524	√			
1463.820	√	√		√
1465.895		√		√
1490.626	√			
1491.854	√			√
1493.766		√	√	
1511.662	√			
1512.704			√	
1513.777	√		√	√
1515.816				√
1517.757		√	√	√
1518.697	√			
1519.876		√	√	√
1538.903		√		
1540.835	√	√	√	√
1546.881	√	√	√	√
1562.233				√
1563.379			√	
1565.841	√	√	√	√
1571.983				√
1573.041			√	
1586.826				√
1588.886	√		√	
1592.098	√	√		√

Detected metabolite ion signals [a] (*m/z*)	Atlantic salmon eyeball tissue sections			
	OCT-embedding	Agarose-embedding	Gelatin-embedding	PAAG-embedding
1594.593	√	√	√	
1597.955		√		
1613.495	√	√		
1615.614			√	√
1621.258		√		
1637.710				√
1639.442		√	√	
1639.615		√	√	
1685.375		√		
Total number of detected compounds	138	161	158	195

a) Detected metabolite ion signal data were duplicate values obtained from three parallel detection of each group (n=3×3).

Table S5. Comparison of metabolite ion signals detected in the tissue sections of Atlantic salmon eyeballs embedded with OCT, agarose, gelatin, and PAAG, respectively, by (-)MALDI-TOF/TOF MS using MEK as the matrix (n=3×3).

Detected metabolite ion signals [a] (*m/z*)	Atlantic salmon eyeball tissue sections			
	OCT-embedding	Agarose-embedding	Gelatin-embedding	PAAG-embedding
104.078				
111.027	√		√	√
113.024	√	√	√	√
119.981	√			√
122.019	√			√
123.022	√			√
124.041	√	√	√	√
125.044	√			√
130.123				
132.076	√			√
132.910	√			√
134.058	√		√	√
135.045	√		√	√
137.065		√		
138.057	√	√		√
140.047	√			√
145.109	√	√		√
146.097	√	√	√	√
147.006	√			√
148.126	√	√	√	√
150.071	√	√	√	√
152.049	√	√	√	√
153.049	√	√	√	√
154.081	√	√	√	√
155.024		√		
158.048	√		√	√
159.060	√		√	√
164.129				
166.025	√	√	√	√
168.042	√	√	√	√
170.978		√		
174.092	√			√

Detected metabolite ion signals [a] (*m/z*)	Atlantic salmon eyeball tissue sections			
	OCT-embedding	Agarose-embedding	Gelatin-embedding	PAAG-embedding
179.066	√	√		√
180.073	√	√		√
182.006	√	√	√	√
184.017	√	√		√
191.057	√	√		√
192.125	√			√
193.035	√	√		√
196.071	√	√	√	√
197.057		√	√	
198.023	√		√	√
207.088	√			√
209.006	√			√
211.039	√	√		√
212.055	√	√	√	√
213.074	√	√	√	√
214.044		√		
215.109			√	
223.082	√	√		√
224.098	√	√	√	√
236.051	√	√		√
241.047		√	√	
245.037			√	
249.069	√	√		√
251.089	√	√	√	√
252.124	√	√	√	√
253.194	√	√	√	√
255.211	√	√	√	√
259.928		√		
263.069	√			√
264.089	√			√
265.099	√	√	√	√
266.116	√	√	√	√
267.119	√	√	√	√
268.125	√		√	√
279.112	√	√	√	√

Detected metabolite ion signals [a] **(*m/z*)**	Atlantic salmon eyeball tissue sections			
	OCT-embedding	Agarose-embedding	Gelatin-embedding	PAAG-embedding
281.190	√	√	√	√
283.208	√	√	√	√
291.015	√	√	√	√
292.996	√	√	√	√
295.107	√	√	√	√
296.244	√	√	√	√
301.262	√	√	√	√
303.263	√	√	√	√
307.214	√	√		√
309.208	√	√	√	√
311.189	√		√	√
321.189	√	√	√	√
323.210	√	√	√	√
325.236	√	√	√	√
327.232	√	√	√	√
329.251	√	√	√	√
330.203	√			√
330.931	√			√
331.684	√			√
337.205	√		√	√
339.211	√	√	√	√
349.227	√	√		√
351.215	√			√
353.256	√	√	√	√
354.926			√	
355.192	√	√	√	√
357.114				
369.169	√	√		√
371.187	√		√	√
375.164	√			√
381.197				
383.174	√		√	√
385.192	√	√	√	√
387.180	√		√	√
391.215	√	√	√	√

Detected metabolite ion signals [a] (*m/z*)	Atlantic salmon eyeball tissue sections			
	OCT-embedding	Agarose-embedding	Gelatin-embedding	PAAG-embedding
393.070	√		√	√
394.111		√		
395.059	√	√	√	√
397.181				
399.186	√		√	√
409.227	√	√		√
414.241	√	√	√	√
417.193	√	√	√	√
419.240	√	√	√	√
425.176	√		√	√
428.247	√			√
429.229	√			√
431.218	√	√	√	√
435.239	√		√	√
437.250	√	√	√	√
441.220				
442.258	√	√	√	√
447.239	√	√		√
452.260	√		√	√
457.237	√		√	√
459.168		√		
460.162				
461.161		√		
462.273	√		√	√
463.221	√	√	√	√
464.277	√		√	√
465.217	√			√
467.352	√	√	√	√
470.272	√	√	√	√
472.281	√	√	√	√
474.234	√	√	√	√
475.213	√		√	√
478.275	√	√	√	√
480.280	√	√	√	√
481.208	√	√	√	√

Detected metabolite ion signals [a] (*m/z*)	Atlantic salmon eyeball tissue sections			
	OCT-embedding	Agarose-embedding	Gelatin-embedding	PAAG-embedding
483.228	√			√
485.250				
490.269	√		√	√
498.282	√		√	√
500.267	√		√	√
502.248	√	√		√
503.163		√		
504.234	√		√	√
505.172		√	√	
506.262	√		√	√
507.211	√	√	√	√
509.213		√		
514.265	√		√	√
518.285	√	√	√	√
519.224		√		
521.241		√		
524.274	√	√	√	√
529.242				
531.235		√		
533.291	√	√	√	√
535.214	√	√	√	√
537.218	√	√		√
546.312	√	√	√	√
548.334	√		√	√
552.273	√		√	√
553.182	√		√	√
568.218	√		√	√
574.320	√		√	√
576.347	√	√	√	√
582.268	√		√	√
587.353	√		√	√
589.357	√	√	√	√
590.276	√		√	√
595.201	√	√	√	√
603.367	√		√	√

Detected metabolite ion signals [a] (*m/z*)	Atlantic salmon eyeball tissue sections			
	OCT-embedding	Agarose-embedding	Gelatin-embedding	PAAG-embedding
605.384	√		√	√
613.353	√	√	√	√
615.389	√	√	√	√
617.403	√	√	√	√
619.417	√	√	√	√
622.371	√			√
631.417		√		
643.403	√	√	√	√
645.425	√	√	√	√
647.435	√	√	√	√
649.429	√	√	√	√
650.967		√		
651.443	√	√		√
653.462		√		
659.492	√		√	√
671.459	√		√	√
673.483	√	√	√	√
675.973		√		
677.468		√		
686.465				
688.482				
693.447	√		√	√
698.507	√			√
699.509	√	√	√	√
700.529	√			√
701.489	√		√	√
702.533	√			√
714.503	√			√
716.517	√		√	√
719.471	√	√	√	√
721.476	√		√	√
724.509				
726.549	√			√
728.560	√		√	√
731.515	√		√	√

Detected metabolite ion signals [a] (*m/z*)	Atlantic salmon eyeball tissue sections			
	OCT-embedding	Agarose-embedding	Gelatin-embedding	PAAG-embedding
736.488	√		√	√
738.495	√		√	√
740.474				
742.534	√		√	√
743.091		√		
744.551	√	√	√	√
745.482	√	√	√	√
746.535	√	√	√	√
747.526	√	√	√	√
748.545	√		√	√
750.511	√		√	√
758.523	√		√	√
762.513	√	√	√	√
764.540	√		√	√
766.542	√	√	√	√
770.548	√		√	√
771.527		√		
772.555	√		√	√
773.547	√		√	√
774.551	√	√	√	√
775.543	√			√
776.526	√		√	√
778.563	√		√	√
786.487	√		√	√
788.528	√		√	√
790.558	√	√	√	√
792.552	√	√		√
797.679				
802.527		√	√	
804.543	√	√	√	√
807.545	√			√
808.543	√		√	√
809.562	√			√
810.533	√		√	√
814.517	√		√	√

Detected metabolite ion signals [a] **(*m/z*)**	Atlantic salmon eyeball tissue sections			
	OCT-embedding	Agarose-embedding	Gelatin-embedding	PAAG-embedding
816.565	√	√	√	√
818.579	√	√	√	√
821.542	√			√
822.558	√		√	√
828.533	√		√	√
832.544	√			√
833.561	√		√	√
834.550	√	√	√	√
835.585	√		√	√
836.538	√	√	√	√
846.501	√		√	√
848.543	√		√	√
850.503			√	
856.553	√	√	√	√
857.562	√	√	√	√
860.641	√	√	√	√
862.603	√	√	√	√
863.637	√	√	√	√
876.570	√	√	√	√
878.486	√		√	√
881.543	√			√
883.569	√	√	√	√
885.587	√	√	√	√
888.679	√		√	√
892.493			√	
894.519	√		√	√
900.502	√	√	√	√
904.664	√			√
909.556	√		√	√
935.490			√	
937.524			√	
939.564	√		√	√
941.581				
981.464			√	
995.562				

Detected metabolite ion signals [a] **(*m/z*)**	Atlantic salmon eyeball tissue sections			
	OCT-embedding	Agarose-embedding	Gelatin-embedding	PAAG-embedding
1002.597			√	
1023.555	√		√	√
1025.595			√	
1069.512	√		√	√
1071.506	√		√	√
1084.501	√			√
1086.489	√		√	√
1097.464	√		√	√
1110.552	√		√	√
1112.437	√		√	√
1114.451	√		√	√
1116.463	√		√	√
1138.361		√	√	
1140.398	√			√
1141.465			√	
1144.479			√	
1156.394	√			√
1157.443			√	
1158.388	√			√
1182.388	√			√
1184.333	√		√	√
1218.291	√			√
1281.242			√	
1424.803	√		√	√
1450.950			√	
1468.777			√	
1470.548	√		√	√
1494.456	√		√	√
1495.973	√		√	√
1499.492	√			√
1516.134	√			√
1541.962	√		√	√
1567.965	√		√	√
1574.236			√	
1587.895	√			√

Detected metabolite ion signals [a] (*m/z*)	Atlantic salmon eyeball tissue sections			
	OCT-embedding	Agarose-embedding	Gelatin-embedding	PAAG-embedding
1614.106			√	
Total number of detected compounds	143	211	210	253

a) Detected metabolite ion signal data were duplicate values obtained from three parallel detection of each group (n=3×3).

Table S6. Metabolites detected and assigned in PAAG embedded Atlantic salmon eyeball tissue sections by (+)MALDI-TOF/TOF MS using 2-MBT as the matrix.

No.	Measured *m/z*	Calculated *m/z*	Error |ppm|	Assignment			Structurally specific CID ions (*m/z*) [a)]
				Ion form	Compound	Molecular formula	
1	104.345	-	-	-	-	-	
2	132.182	-	-	-	-	-	
3	136.104	-	-	-	-	-	
4	147.038	-	-	-	-	-	
5	156.107	-	-	-	-	-	
6	166.066	166.0661	1	$[M+Na]^+$	2-Ethyl-2,5-dihydro-4,5-dimethylthiazole	$C_7H_{13}NS$	41, 56
7	166.977	166.9773	2	$[M+K]^+$	2-Amino-5-chloropyridine	$C_5H_5ClN_2$	75, 129 66, 85, 100, 129
8	167.993	167.9936	4	$[M+H]^+$	2(3H)-Benzothiazolethione	$C_7H_5NS_2$	51, 109
9	169.018	169.0174	4	$[M+H]^+$	Ethyl propyl trisulfide	$C_5H_{12}S_3$	45, 61
10	170.008	170.0069	7	$[M+Na]^+$	Ibervirin	$C_5H_9NS_2$	41, 89
11	184.057	184.0580	6	$[M+Na]^+$	3-Aminoadipic acid	$C_6H_{11}NO_4$	42, 70
12	189.979	189.9780	5	$[M+K]^+$	1-(2-Chloroethyl)-1-nitrosourea	$C_3H_6ClN_3O_2$	63, 109 44, 63, 73
13	191.972	191.9727	4	$[M+K]^+$	3-Sulfinoalanine	$C_3H_7NO_4S$	42, 81, 108
14	198.067	198.0680	5	$[M+H]^+$	Clephedrone	$C_{10}H_{12}ClNO$	51, 111, 164
15	199.944	199.9431	5	$[M+K]^+$	Dichloroaniline	$C_6H_5Cl_2N$	39, 85, 162
16	205.947	-	-	-	-	-	
17	211.945	-	-	-	-	-	
18	227.913	-	-	-	-	-	
19	238.995	238.9952	1	$[M+K]^+$	Maleylacetoacetic acid	$C_8H_8O_6$	61, 71, 87, 99, 155
20	243.889	-	-	-	-	-	
21	253.038	253.0374	2	$[M+K]^+$	4-(4-Nitrobenzyl)pyridine	$C_{12}H_{10}N_2O_2$	84, 132, 211
22	256.987	256.9856	6	$[M+K]^+$	Diphenyl disulfide	$C_{12}H_{10}S_2$	51, 83, 109,
23	258.080	258.0795	2	$[M+H]^+$	2-(Ethyl sulfonylmethyl)phenyl methylcarbamate	$C_{11}H_{15}NO_4S$	58, 93, 155, 171
24	259.015	259.0149	4	$[M+K]^+$	N-Acetyl-S-(N-methylcarbamoyl)cysteine	$C_7H_{12}N_2O_4S$	60, 84, 116
25	269.003	-	-	-	-	-	
26	270.010	270.0083	6	$[M+K]^+$	2-Amino-5-chlorobenzophenone	$C_{13}H_{10}ClNO$	51, 105, 154
27	275.967	-	-	-	-	-	
28	279.080	279.0798	1	$[M+H]^+$	5-hydroxyindole thiazolidine carboxylate	$C_{13}H_{14}N_2O_3S$	132, 146, 173

No.	Measured *m/z*	Calculated *m/z*	Error |ppm|	Assignment			Structurally specific CID ions (*m/z*) [a]
				Ion form	Compound	Molecular formula	
29	280.079	280.0803	3	$[M+K]^+$	Tetrahydrobiopterin	$C_9H_{15}N_5O_3$	55, 124, 149, 166
30	290.997	290.9950	7	$[M+Na]^+$	Dichlorophen	$C_{13}H_{10}Cl_2O_2$	111, 141, 251
31	296.063	296.0643	4	$[M+K]^+$	2'-C-Methylcytidine	$C_{10}H_{15}N_3O_5$	95, 112, 130
32	300.986	300.9866	2	$[M+K]^+$	Dehydro-4-methoxycyclobrassinin	$C_{12}H_{10}N_2OS_2$	47, 231 47, 127, 171, 231
33	302.996	302.9935	8	$[M+K]^+$	3-Methoxy-4-hydroxyphenylethyleneglycol sulfate	$C_9H_{12}O_7S$	51, 81, 137, 203
34	312.364	-	-	-	-	-	
35	322.976	322.9766	2	$[M+K]^+$	Sulfachlorpyridazine	$C_{10}H_9ClN_4O_2S$	68, 88, 130
36	332.962	332.9643	7	$[M+H]^+$	2,2'-Dithiobisbenzothiazole	$C_{14}H_8N_2S_4$	51, 109
37	334.004	334.0008	10	$[M+Na]^+$	3'-Hydroxydiclofenac	$C_{14}H_{11}Cl_2NO_3$	77, 266
38	334.980	-	-	-	-	-	
39	336.979	336.9808	5	$[M+Na]^+$	Iodoantipyrine	$C_{11}H_{11}IN_2O$	92, 120, 167, 196
40	346.995	346.9986	10	$[M+K]^+$	2-Hydroxy-4-methoxybenzophenone sulfate	$C_{14}H_{12}O_6S$	77, 105, 151, 283
41	354.981	354.9785	7	$[M+H]^+$	5'-Iododeoxyuridine	$C_9H_{11}IN_2O_5$	42, 223
42	356.982	356.9806	4	$[M+K]^+$	(2R,3R,4S,5R)-2-(5,6-Dichlorobenzimidazol-1-yl)-5-(hydroxymethyl)oxolane-3,4-diol	$C_{12}H_{12}Cl_2N_2O_4$	153, 187, 199
43	364.941	-	-	-	-	-	
44	366.939	-	-	-	-	-	
45	370.943	-	-	-	-	-	
46	386.955	386.9571	6	$[M+K]^+$	Daidzein sulfate	$C_{15}H_8O_8S$	316, 349
47	390.047	390.0463-	2	$[M+Na]^+$	Lodoxamide ethyl	$C_{15}H_{14}ClN_3O_6$	47, 168, 240, 368
48	392.066	392.0651	2	$[M+Na]^+$	Lansoprazole	$C_{16}H_{14}F_3N_3O_2S$	184, 252
49	396.910	396.9133	8	$[M+K]^+$	Triclabendazole	$C_{14}H_9Cl_3N_2OS$	47, 359 47, 85, 147, 213, 359
50	398.909	-	-	-	-	-	
51	400.402	-	-	-	-	-	
52	400.904	-	-	-	-	-	
53	404.043	404.0427	1	$[M+Na]^+$	Dehydrofelodipine	$C_{18}H_{17}Cl_2NO_4$	164, 250, 276,
54	406.075	406.0720	7	$[M+H]^+$	Difenoconazole	$C_{19}H_{17}Cl_2N_3O_3$	141, 188, 223, 251

No.	Measured *m/z*	Calculated *m/z*	Error |ppm|	Assignment			Structurally specific CID ions (*m/z*) a)
				Ion form	Compound	Molecular formula	
55	424.038	424.0400	5	$[M+H]^+$	Glucoiberin	$C_{11}H_{21}NO_{10}S_3$	261, 406, 424
56	426.412	-	-	-	-	-	
57	428.455	-	-	-	-	-	
58	440.913	-	-	-	-	-	
59	442.889	-	-	-	-	-	
60	456.026	-	-	-	-	-	
61	466.022	466.0252	7	$[M+K]^+$	Cefpodoxime	$C_{15}H_{17}N_5O_6S_2$	56, 188, 243, 366
62	468.013	-	-	-	-	-	
63	468.420	-	-	-	-	-	
64	478.419	-	-	-	-	-	
65	482.415	-	-	-	-	-	
66	494.328	494.3241	8	$[M+H]^+$	LPC(16:1)	$C_{24}H_{48}NO_7P$	104, 311, 441
67	496.375	496.3761	3	$[M+H]^+$	LPC(O-17:0)	$C_{25}H_{54}NO_6P$	480, 391, 168, 97
68	497.992	497.9951	6	$[M+Na]^+$	2',3'-Dideoxyadenosine-5-triphosphate	$C_{10}H_{16}N_5O_{11}P_3$	81, 136, 218, 378
69	499.983	-	-	-	-	-	
70	504.435	504.4387	7	$[M+Na]^+$	Cer(d30:1)	$C_{30}H_{59}NO_3$	264, 282, 464
71	508.482	-	-	-	-	-	
72	515.113	515.1165	7	$[M+Na]^+$	Malvidin 3-glucoside	$C_{23}H_{25}O_{12}$	103, 163, 315, 331, 493
73	518.379	518.3816	5	$[M+Na]^+$	N-Nervonoyl Glutamic acid	$C_{29}H_{53}NO_5$	43, 100, 123, 148, 360
74	522.396	522.3919	8	$[M+K]^+$	Docosanoylcarnitine	$C_{29}H_{57}NO_4$	71, 85, 425
75	524.408	524.4075	1	$[M+H]^+$	Edelfosine	$C_{27}H_{58}NO_6P$	88, 253, 341, 508
76	525.117	502.1271	1	$[M+Na]^+$	Fluvalinate	$C_{26}H_{22}ClF_3N_2O_3$	51, 132, 226, 278, 477
77	529.960	529.9640	8	$[M+K]^+$	Deoxyadenosine triphosphate	$C_{10}H_{16}N_5O_{12}P_3$	94, 109, 136, 357
78	531.924	-	-	-	-	-	
79	534.360	534.3554	9	$[M+H]^+$	LPE(22:2)	$C_{27}H_{52}NO_7P$	44, 151, 319, 377, 422
80	540.991	-	-	-	-	-	
81	544.380	-	-	-	-	-	
82	557.088	557.0902	4	$[M+Na]^+$	3,5-Dihydroxy-3',4'-dimethoxy-6,7-methylenedioxyflavone 3-glucuronide	$C_{24}H_{22}O_{14}$	87, 181, 343, 359, 505
83	561.911	-	-	-	-	-	

No.	Measured *m/z*	Calculated *m/z*	Error |ppm|	Assignment			Structurally specific CID ions (*m/z*) [a)]
				Ion form	Compound	Molecular formula	
84	568.374	568.3763	4	$[M+K]^+$	N-Nervonoyl Tyrosine	$C_{33}H_{55}NO_4$	83, 109, 136, 424
85	573.926	-	-	-	-	-	
86	589.041	589.0442	5	$[M+Na]^+$	Uridine diphosphate glucose	$C_{15}H_{24}N_2O_{17}P_2$	57, 113, 227, 387, 405
87	590.362	590.3582	6	$[M+K]^+$	LPC(20:0)	$C_{28}H_{58}NO_7P$	59, 88, 197, 267, 295, 369
88	606.349	606.3471	3	$[M+H]^+$	Dynorphin B (6-9)	$C_{26}H_{43}N_{11}O_6$	60, 101, 129, 285, 354, 533
89	614.266	614.2721	10	$[M+H]^+$	Ferrioxamine B	$C_{25}H_{45}F_eN_6O_8$	86, 614 41, 72, 86, 485, 541
90	615.253	-	-	-	-	-	
91	616.275	616.2783	5	$[M+K]^+$	Aplaviroc	$C_{33}H_{43}N_3O_6$	57, 381, 578
92	617.329	617.3351	10	$[M+K]^+$	Deoxycholyltryptophan	$C_{35}H_{50}N_2O_5$	118, 375, 579 97, 118, 167, 375, 533, 579
93	630.278	630.2738	7	$[M+K]^+$	Fluphenazine decanoate	$C_{32}H_{44}F_3N_3O_2S$	81, 153, 213, 420, 590
94	631.265	631.2628	3	$[M+K]^+$	Hexobendine	$C_{30}H_{44}N_2O_{10}$	86, 171, 255, 349, 593
95	632.270	-	-	-	-	-	
96	638.259	-	-	-	-	-	
97	639.247	639.2449	3	$[M+H]^+$	Hexyl heptanoate	$C_{35}H_{34}N_4O_8$	63, 107, 120, 327, 533
98	646.279	646.2769	3	$[M+Na]^+$	Leukotriene C5	$C_{30}H_{45}N_3O_9S$	56, 177, 333, 475, 560
99	648.260	648.2583	3	$[M+K]^+$	Ergocristine	$C_{35}H_{39}N_5O_5$	70, 98, 166, 223, 334
100	655.066	-	-	-	-	-	
101	675.524	675.5194	7	$[M+H]^+$	DG(18:0/PGJ2)	$C_{41}H_{70}O_7$	307, 357, 363, 413, 697
102	676.593	-	-	-	-	-	
103	678.615	-	-	-	-	-	
104	683.972	-	-	-	-	-	
105	697.504	697.5014	4	$[M+Na]^+$	DG(18:0/ PGJ2)	$C_{41}H_{70}O_7$	307, 357, 363, 413, 698
106	698.561	698.5565	6	$[M+H]^+$	N-[(4E,8Z)-1,3-dihydroxyoctadeca-4,8-dien-2-yl]hexadecanamide 1-glucoside	$C_{40}H_{75}NO_8$	43, 127, 211, 440, 518, 663

No.	Measured *m/z*	Calculated *m/z*	Error |ppm|	Assignment			Structurally specific CID ions (*m/z*) a)
				Ion form	Compound	Molecular formula	
107	700.601	-	-	-	-	-	
108	704.623	-	-	-	-	-	
109	706.644	-	-	-	-	-	
110	711.924	-	-	-	-	-	
111	714.558	714.5515	9	$[M+H]^+$	Soyacerebroside I	$C_{40}H_{75}NO_9$	43, 163, 278, 458, 656
112	716.587	-	-	-	-	-	
113	718.630	-	-	-	-	-	
114	724.579	724.5850	8	$[M+Na]^+$	Arachidyl amido cholanoic acid	$C_{44}H_{79}NO_5$	41, 93, 295, 434, 518, 703
115	726.612	-	-	-	-	-	
116	728.620	-	-	-	-	-	
117	730.580	730.5745	8	$[M+H]^+$	PE(P-36:1)	$C_{41}H_{80}NO_7P$	44, 307, 688 44, 142, 267, 307, 421, 575
118	732.625	-	-	-	-	-	
119	739.998	-	-	-	-	-	
120	742.568	742.5745	9	$[M+H]^+$	PC(O-34:3)	$C_{42}H_{80}NO_7P$	279, 375, 464, 655, 715
121	744.592	744.5902	2	$[M+H]^+$	PC(P-34:1)	$C_{42}H_{82}NO_7P$	88, 249, 323, 490, 550, 630, 701
122	746.575	746.5694	7	$[M+H]^+$	PE(36:1)	$C_{41}H_{80}NO_8P$	285, 395, 408, 426, 536, 605, 728
123	752.588	752.5928	6	$[M+Na]^+$	CerP(d42:1)	$C_{42}H_{84}NO_6P$	55, 95, 265, 365, 617
124	754.618	754.6109	9	$[M+H]^+$	PC(P-36:2)	$C_{44}H_{84}NO_6P$	88, 249, 572 88, 249, 307, 490, 570, 683
125	756.574	-	-	-	-	-	
126	758.574	758.5694	-	$[M+H]^+$	PC(34:2)	$C_{42}H_{80}NO_8P$	86, 699
127	760.583	760.5851	3	$[M+H]^+$	PC(34:1)	$C_{42}H_{82}NO_8P$	86, 577, 761
128	766.570	766.5721	3	$[M+Na]^+$	PC(P-34:1)	$C_{42}H_{82}NO_7P$	88, 249, 480, 658, 701
129	768.588	768.5878	0	$[M+Na]^+$	PC(O-34:1)	$C_{42}H_{84}NO_7P$	88, 184, 267, 297, 550, 689
130	770.598	770.6034	7	$[M+Na]^+$	PC(O-34:0)	$C_{42}H_{86}NO_7P$	72, , 299, 691
131	772.616	772.6215	7	$[M+H]^+$	PC(P-36:1)	$C_{44}H_{86}NO_7P$	88, 590

No.	Measured *m/z*	Calculated *m/z*	Error |ppm|	Assignment: Ion form	Assignment: Compound	Assignment: Molecular formula	Structurally specific CID ions (*m/z*) a)
132	774.620	-	-	-	-	-	88, 249, 403, 506, 590, 755
133	780.547	780.5514	6	$[M+Na]^+$	PC(34:2)	$C_{42}H_{80}NO_8P$	88, 291, 741 88, 169, 291, 365, 566, 715
134	782.596	782.6034	7	$[M+Na]^+$	PE(P-38:0)	$C_{43}H_{86}NO_7P$	79, 311, 603
135	786.618	786.6233	7	$[M+K]^+$	Tetrac	$C_{14}H_8I_4O_4$	371, 577
136	788.635	-	-	-	-	-	
137	792.573	792.5668	2	$[M+H]^+$	PS(36:0)	$C_{42}H_{82}NO_{10}P$	44, 734 192, 490, 608, 712,
138	794.608	794.6058	3	$[M+H]^+$	PC(P-38:4)	$C_{46}H_{84}NO_7P$	79, 237, 305, 441, 689
139	798.582	798.5773	6	$[M+K]^+$	PE(P-38:0)	$C_{43}H_{86}NO_7P$	42, 703
140	804.382	-	-	-	-	-	
141	806.538	806.5330	-	$[M+H]^+$	PE(40:7)	$C_{45}H_{76}NO_9P$	164, 471, 479
142	808.581	808.5827	1	$[M+Na]^+$	PC(36:2)	$C_{44}H_{84}NO_8P$	147, 467, 526, 544, 626, 750
143	810.627	810.6347	9	$[M+Na]^+$	PE(P-40:0)	$C_{45}H_{90}NO_7P$	44, 381, 634
144	813.667	813.6603	8	$[M+H]^+$	Isofucosterol 3-O-[6-O-Hexadecanoyl-b-D-glucopyranoside]	$C_{51}H_{88}O_7$	97, 147, 239, 413, 657, 714
145	818.537	818.5330	5	$[M+H]^+$	PC(38:8)	$C_{46}H_{76}NO_9P$	86, 104, 125, 184, 500, 558, 635
146	824.592	824.5930	1	$[M+K]^+$	PE(P-40:1)	$C_{45}H_{88}NO_7P$	44, 57, 142, 198, 309, 466
147	826.646	-	-	-	-	-	
148	828.542	828.5445	3	$[M+Na]^+$	LacCer(d30:1)	$C_{42}H_{79}NO_{13}$	264, 447, 807
149	830.540	830.5460	7	$[M+K]^+$	PC(P-38:5)	$C_{46}H_{82}NO_7P$	88, 249, 610 88, 249, 323, 490, 596, 692, 749
150	832.565	832.5617	4	$[M+K]^+$	PC(P-38:4)	$C_{46}H_{84}NO_7P$	86, 104, 124 ,184, 267
151	834.555	834.5619	8	$[M+Na]^+$	PE(40:4-OH)	$C_{45}H_{82}NO_9P$	351, 672 351, 492, 672, 795, 813
152	835.626	835.6212	6	$[M+K]^+$	TG(48:5)	$C_{51}H_{88}O_6$	309, 804

No.	Measured *m/z*	Calculated *m/z*	Error |ppm|	Assignment			Structurally specific CID ions (*m/z*) a)
				Ion form	Compound	Molecular formula	
153	842.549	842.5542	6	$[M+H]^+$	PE(40:5-3OH)	$C_{45}H_{80}NO_{11}P$	367, 490, 550, 702, 825
154	844.514	844.5123	2	$[M+H]^+$	PE(42:10)	$C_{47}H_{74}NO_{10}P$	164, 463, 519, 725, 823, 866
155	846.542	846.5410	1	$[M+K]^+$	PC(38:5)	$C_{46}H_{82}NO_8P$	86, 104, 125, 184, 478, 496, 570, 626, 750
156	854.568	854.5670	1	$[M+Na]^+$	PC(40:7)	$C_{48}H_{82}NO_8P$	88, 219, 323, 506, 650, 760
157	856.520	856.5253	6	$[M+K]^+$	PE(42:7)	$C_{47}H_{80}NO_8P$	367, 385, 508, 526, 678, 801
158	863.558	863.5563	2	$[M+K]^+$	PA(44:4)	$C_{47}H_{85}O_9P$	479, 497, 527, 545, 727, 710
159	872.571	-	-	-	-	-	
160	878.427	878.4285	2	$[M+K]^+$	Ala-Thr-Trp-Leu-Pro-Pro-Arg	$C_{40}H_{61}N_{11}O_9$	44, 74, 130, 260, 265, 373, 567, 624
161	925.515	925.5203	6	$[M+K]^+$	PI(38:4)	$C_{47}H_{83}O_{13}P$	41,165, 211, 297, 409, 627, 717, 869
162	927.482	927.4841	2	$[M+Na]^+$	PI(40:9)	$C_{45}H_{77}O_{16}P$	97, 223, 315, 413, 481, 593, 643, 904
163	947.988	-	-	-	-	-	
164	973.418	973.4251	7	$[M+Na]^+$	Rebaudioside C	$C_{44}H_{70}O_{22}$	87, 147, 317, 481, 641, 771, 933
165	1231.072	-	-	-	-	-	
166	1279.668	-	-	-	-	-	
167	1281.670	-	-	-	-	-	
168	1347.332	-	-	-	-	-	
169	1373.335	-	-	-	-	-	
170	1375.430	-	-	-	-	-	
171	1396.208	-	-	-	-	-	
172	1402.442	-	-	-	-	-	
173	1409.663	-	-	-	-	-	
174	1421.390	-	-	-	-	-	
175	1433.733	-	-	-	-	-	

No.	Measured *m/z*	Calculated *m/z*	Error |ppm|	Assignment			Structurally specific CID ions (*m/z*) a)
				Ion form	Compound	Molecular formula	
176	1435.665	1435.6587	4	$[M+H]^+$	Capsicoside E	$C_{64}H_{106}O_{35}$	163, 325, 487, 625, 947, 1110, 1256, 1418
177	1437.873	1437.8832	7	$[M+Na]^+$	Ganglioside GM2 (d40:2)	$C_{72}H_{128}N_2O_{26}$	57, 142, 221, 364, 438, 587, 1116, 1438
178	1457.688	-	-	-	-	-	
179	1461.148	-	-	-	-	-	
180	1463.820	1463.8104	6	$[M+H]^+$	Ganglioside GM1 (d30：0)	$C_{68}H_{122}N_2O_{31}$	45, 95, 163, 309, 438, 656, 1265, 1464
181	1465.895	-	-	-	-	-	
182	1491.854	1491.8417	8	$[M+H]^+$	Ganglioside GM1 (d32:0)	$C_{70}H_{126}N_2O_{31}$	57, 163, 383, 478, 762, 998, 1265, 1402
183	1513.777	-	-	-	-	-	
184	1515.816	-	-	-	-	-	
185	1517.757	-	-	-	-	-	
186	1519.876	1519.8730	2	$[M+H]^+$	Ganglioside GM1 (d34:0)	$C_{72}H_{130}N_2O_{31}$	81, 163, 383, 438, 656, 762, 1280
187	1540.835	1540.8346	0	$[M+Na]^+$	Ganglioside GM1 (34:1)	$C_{71}H_{127}N_3O_{31}$	165, 282, 366, 438, 506, 657, 999, 1518
188	1546.881	1546.8839	2	$[M+H]^+$	Ganglioside GM1 (36:1)	$C_{73}H_{131}N_3O_{31}$	95, 163, 282, 438, 657, 1388, 1547
189	1562.233	-	-	-	-	-	
190	1565.841	1565.8550	9	$[M+Na]^+$	Ganglioside GM1 (36:2)	$C_{74}H_{130}N_2O_{31}$	81, 138, 163, 438, 530, 656, 762, 1454
191	1571.983	1571.9952	8	$[M+H]^+$	CL(82:17)	$C_{91}H_{144}O_{17}P_2$	265, 385, 539, 672, 828, 988, 1230, 1308, 1554
192	1586.826	-	-	-	-	-	
193	1592.098	-	-	-	-	-	
194	1615.614	-	-	-	-	-	
195	1637.710	-	-	-	-	-	

a) Structurally specific CID ions of extracted compounds were detected by LC-MS/MS and/or MALD-TOF/TOF MS/MS using CID. Red fragment ions were detected by LC-MS/MS, and blue fragment ions were detected by MALDI-TOF/TOF MS/MS.

Table S7. Metabolites detected and assigned in PAAG embedded Atlantic salmon eyeball tissue sections by (−)MALDI-TOF/TOF MS using MEK as the matrix.

No.	Measured *m/z*	Calculated *m/z*	Error |ppm|	Assignment			Structurally specific CID ions (*m/z*) [a]
				Ion form	Compound	Molecular formula	
1	111.027	-	-	-	-	-	
2	113.024	113.0244	4	$[M-H]^-$	cis-Acetylacrylate	$C_5H_6O_3$	43, 51, 69
3	119.981	-	-	-	-	-	
4	122.019	-	-	-	-	-	
5	123.022	-	-	-	-	-	
6	124.041	124.0404	5	$[M-H]^-$	5-(Hydroxymethyl)-1H-pyrrole-2-carbaldehyde	$C_6H_7NO_2$	66, 124 66, 92, 124
7	125.044	-	-	-	-	-	
8	132.076	-	-	-	-	-	
9	132.910	-	-	-	-	-	
10	134.058	-	-	-	-	-	
11	135.045	135.0452	1	$[M-H]^-$	M-toluic Acid	$C_8H_8O_2$	65, 91, 135
12	138.057	138.0561	7	$[M-H]^-$	3,4-Dihydroxybenzylamine	$C_7H_9NO_2$	41, 51, 66
13	140.047	140.0466	3	$[M-H]^-$	Dimetridazole	$C_5H_7N_3O_2$	42, 73, 99, 130
14	145.109	-	-	-	-	-	
15	146.097	146.0975	3	$[M-H]^-$	1,2,3,4-Tetrahydro-2-naphthylamine	$C_{10}H_{13}N$	77, 91, 129
16	147.006	-	-	-	-	-	
17	148.126	-	-	-	-	-	
18	150.071	-	-	-	-	-	
19	152.049	152.0484	4	$[M-H]^-$	(2E)-4-hydroxy-5-methyl-2-propylidene-3(2H)-furanone	$C_8H_9O_3$	55, 135, 137
20	153.049	-	-	-	-	-	
21	154.081	-	-	-	-	-	
22	158.048	158.0472	5	$[M-H]^-$	1,N6-Ethenoadenine	$C_7H_5N_5$	89, 131, 158
23	159.060	-	-	-	-	-	
24	166.025	-	-	-	-	-	
25	168.042	168.0431	7	$[M-H]^-$	Phosphodimethylethanolamine	$C_4H_{12}NO_4P$	63,79, 97
26	174.092	174.0924	3	$[M-H]^-$	Dimethylaminocinnamaldehyde	$C_{11}H_{13}NO$	44, 91, 132
27	179.066	179.0648	6	$[M-H]^-$	Protionamide	$C_7H_{14}FO_2P$	33, 58, 120
28	180.073	-	-	-	-	-	
29	182.006	182.0046	8	$[M-H]^-$	Acephate	$C_4H_{10}NO_3PS$	46, 94, 131
30	184.017	-	-	-	-	-	
31	191.057	-	-	-	-	-	
32	192.125	192.1255	2	$[M-H]^-$	Alvameline	$C_9H_{15}N_5$	40, 92, 121
33	193.035	193.0354	2	$[M-H]^-$	3-Dehydro-L-gulonate	$C_6H_{10}O_7$	57, 59, 87, 117
34	196.071	196.0728	9	$[M-H]^-$	N-Acetylhistidine	$C_8H_{11}N_3O_3$	42, 67, 84, 108
35	198.023	-	-	-	-	-	
36	207.088	207.0874	3	$[M-H]^-$	Ethyl beta-D-glucopyranoside	$C_8H_{16}O_6$	43, 59, 89, 135

No.	Measured *m/z*	Calculated *m/z*	Error |ppm|	Assignment			Structurally specific CID ions (*m/z*) [a]
				Ion form	Compound	Molecular formula	
37	209.006	-	-	-	-	-	
38	211.039	211.0401	5	$[M-H]^-$	Urolithin B	$C_{13}H_8O_3$	141, 169, 183
39	212.055	212.0564	7	$[M-H]^-$	Droxidopa	$C_9H_{11}NO_5$	56, 72, 109, 151
40	213.074	-	-	-	-	-	
41	223.082	223.0837	7	$[M-H]^-$	Temurin	$C_9H_{12}N_4O_3$	56, 109, 166
42	224.098	-	-	-	-	-	
43	236.051	236.0533	10	$[M-H]^-$	Mergepta	$C_7H_{15}N_3O_2S_2$	32, 74, 101
44	249.069	249.0703	5	$[M-H]^-$	Dansylamide	$C_{12}H_{14}N_2O_2S$	79, 154, 206
45	251.089	251.0885	2	$[M-H]^-$	Cycasin	$C_8H_{16}N_2O_7$	44, 206 44, 86, 116, 206
46	252.124	252.1241	1	$[M-H]^-$	L-DOPA n-Butyl Ester	$C_{13}H_{19}NO_4$	72, 123, 179
47	253.194	253.1962	9	$[M-H]^-$	18-Nor-4(19),8,11,13-abietatetraene	$C_{19}H_{26}$	39, 117, 185, 237
48	255.211	-	-	-	-	-	
49	263.069	263.0707	7	$[M-H]^-$	Methionyl-Aspartate	$C_9H_{16}N_2O_5S$	47, 114, 202
50	264.089	264.0877	5	$[M-H]^-$	N-Phenylacetylglutamic acid	$C_{13}H_{15}NO_5$	41, 91, 102, 128
51	265.099	265.0983	3	$[M-H]^-$	Miroprofen	$C_{16}H_{14}N_2O_2$	221, 249 94, 142, 221, 265
52	266.116	266.1146	5	$[M-H]^-$	4-amino-MX	$C_{12}H_{17}N_3O_4$	17, 266 17, 46, 221, 266
53	267.119	267.1179	4	$[M-H]^-$	3-Methylcholanthrene	$C_{21}H_{16}$	51, 251
54	268.125	-	-	-	-	-	
55	279.112	-	-	-	-	-	
56	281.190	281.1911	4	$[M-H]^-$	Vitamin A2 aldehyde	$C_{20}H_{26}O$	65, 237
57	283.208	283.2067	5	$[M-H]^-$	Vitamin A2	$C_{20}H_{28}O$	43, 65, 133, 237
58	291.015	-	-	-	-	-	
59	292.996	-	-	-	-	-	
60	295.107	295.1088	6	$[M-H]^-$	10-Acetoxy-10,11-dihydro-5h-dibenz[b,f]azepine-5-carboxamide	$C_{17}H_{16}N_2O_3$	41, 208
61	296.244	-	-	-	-	-	
62	301.262	-	-	-	-	-	
63	303.263	-	-	-	-	-	
64	307.214	307.2140	0	$[M-H]^-$	2,2'-Azobis(4-methoxy-2,4-dimethylvaleronitrile)	$C_{16}H_{28}N_4O_2$	71, 168, 219, 291

No.	Measured *m/z*	Calculated *m/z*	Error |ppm|	Assignment			Structurally specific CID ions (*m/z*) [a)]
				Ion form	Compound	Molecular formula	
65	309.208	309.2071	3	$[M-H]^-$	12(13)Ep-9-KODE	$C_{18}H_{30}O_4$	41, 59, 109, 193
66	311.189	311.1877	4	$[M-H]^-$	Granisetron	$C_{18}H_{24}N_4O$	42, 104, 171, 295
67	321.189	-	-	-	-	-	
68	323.210	-	-	-	-	-	
69	325.236	325.2384	7	$[M-H]^-$	Avocadyne 2-acetate	$C_{19}H_{34}O_4$	59, 265 41, 59, 265, 283
70	327.232	327.2330	3	$[M-H]^-$	Docosahexaenoic acid	$C_{22}H_{32}O_2$	59, 309, 327 45, 89, 197, 267, 309
71	329.251	329.2486	7	$[M-H]^-$	Docosapentaenoic acid (22n-3)	$C_{22}H_{34}O_2$	45, 59, 71, 131, 283
72	330.203	-	-	-	-	-	
73	330.931	-	-	-	-	-	
74	331.684	-	-	-	-	-	
75	337.205	337.2020	9	$[M-H]^-$	[6]-Gingerdiol 3-acetate	$C_{19}H_{30}O_5$	41, 59, 195, 279
76	339.211	339.0278	9	$[M-H]^-$	Ethylhydrocupreine	$C_{21}H_{28}N_2O_2$	130, 293
77	349.227	349.2285	4	$[M-H]^-$	(+)-cis-3-Methylfentanyl	$C_{23}H_{30}N_2O$	55, 148, 189, 293
78	351.215	351.2177	8	$[M-H]^-$	prostaglandin	$C_{20}H_{32}O_5$	113, 139, 233, 279, 315
79	353.256	-	-	-	-	-	
80	355.192	355.1915	2	$[M-H]^-$	Piperochromanoic acid	$C_{22}H_{28}O_4$	81, 131, 203, 295
81	369.169	369.1707	5	$[M-H]^-$	Calanolide A	$C_{22}H_{26}O_5$	41, 133, 283, 351
82	371.187	371.1864	2	$[M-H]^-$	Tanabalin	$C_{22}H_{28}O_5$	59, 285, 355
83	375.164	-	-	-	-	-	
84	383.174	-	-	-	-	-	
85	385.192	385.1915	1	$[M-H]^-$	Butyryl timolol	$C_{17}H_{30}N_4O_4S$	74, 143, 257, 355
86	387.180	387.1813	3	$[M-H]^-$	Cyclomammein	$C_{22}H_{28}O_6$	41, 67, 301
87	391.215	391.2126	6	$[M-H]^-$	Neuroprostane	$C_{22}H_{32}O_6$	95, 109, 219, 237
88	393.070	393.0668	8	$[M-H]^-$	Diflufenican	$C_{19}H_{11}F_5N_2O_2$	49, 92, 128, 238
89	395.059	-	-	-	-	-	

No.	Measured *m/z*	Calculated *m/z*	Error |ppm|	Assignment			Structurally specific CID ions (*m/z*) [a]
				Ion form	Compound	Molecular formula	
90	399.181	399.1813	1	$[M-H]^-$	Melleolide	$C_{23}H_{28}O_6$	81, 23, 205, 355
91	409.227	409.2232	9	$[M-H]^-$	Forskolin	$C_{22}H_{34}O_7$	59, 139, 243, 349
92	414.241	-	-	-	-	-	
93	417.193	417.1919	3	$[M-H]^-$	Diosbulbin H	$C_{23}H_{30}O_7$	67, 109, 265, 317, 401
94	419.240	-	-	-	-	-	
95	425.176	425.1718	10	$[M-H]^-$	Mespirenone	$C_{25}H_{30}O_4S$	41, 74, 367, 425
96	428.247	428.2442	6	$[M-H]^-$	Mebeverine	$C_{25}H_{35}NO_5$	95, 181, 264, 382
97	429.229	429.2283	2	$[M-H]^-$	Homofukinolide	$C_{25}H_{34}O_6$	55, 99, 235, 317
98	431.218	431.2204	6	$[M-H]^-$	LPA(18:3)	$C_{21}H_{37}O_7P$	
99	435.239	435.2361	7	$[M-H]^-$	DN-isobutylamide	$C_{20}H_{32}N_6O_5$	42, 168, 250, 433
100	437.250	-	-	-	-	-	
101	442.258	-	-	-	-	-	
102	447.239	-	-	-	-	-	
103	452.260	-	-	-	-	-	
104	457.237	457.2674	2	$[M-H]^-$	LPA (18:0)	$C_{21}H_{43}O_7P$	79, 153, 171, 283, 437
105	462.273	462.2762	7	$[M-H]^-$	Bilastine	$C_{28}H_{37}N_3O_3$	45, 157, 272, 390
106	463.221	-	-	-	-	-	
107	464.277	464.2783	3	$[M-H]^-$	LPC (14:1)	$C_{22}H_{44}NO_7P$	210, 225, 486
108	465.217	465.2130	9	$[M-H]^-$	8-Pentanoylneosolaniol	$C_{24}H_{34}O_9$	59, 157, 265, 447
109	467.352	467.3531	2	$[M-H]^-$	Ambonic acid	$C_{31}H_{48}O_3$	55, 73, 341, 451
110	470.272	-	-	-	-	-	
111	472.281	-	-	-	-	-	
112	474.234	474.2362	5	$[M-H]^-$	Fluspirilene	$C_{29}H_{31}F_2N_3O$	42, 95, 173, 324, 415
113	475.213	-	-	-	-	-	
114	478.275	-	-	-	-	-	
115	480.280	480.2755	9	$[M-H]^-$	Dihydrocytochalasin B	$C_{29}H_{39}NO_5$	42, 91, 317, 376, 462

No.	Measured *m/z*	Calculated *m/z*	Error |ppm|	Assignment			Structurally specific CID ions (*m/z*) [a)]
				Ion form	Compound	Molecular formula	
116	481.208	481.2079	0	$[M-H]^-$	3'-Hydroxy-T2 Toxin	$C_{24}H_{34}O_{10}$	41, 183, 321, 381, 463
117	483.228	483.2308	6	$[M-H]^-$	Kanamycin	$C_{18}H_{36}N_4O_{11}$	59, 159, 233, 322, 380
118	490.269	490.2675	3	$[M-H]^-$	Lidoflazine	-	
119	498.282	498.2861	8	$[M-H]^-$	Beloranib	$C_{29}H_{41}NO_6$	119, 163, 303, 411
120	500.267	-	-	-	-	-	
121	502.248	502.2519	8	$[M-H]^-$	Lysyl-aspartyl-glutamyl-leucine	$C_{21}H_{37}N_5O_9$	42, 144, 259, 328, 412
122	504.234	-	-	-	-	-	
123	506.262	506.2582	8	$[M-H]^-$	Epothilone B	$C_{27}H_{41}NO_6S$	40, 74, 138, 472, 486
124	507.211	507.2083	5	$[M-H]^-$	6-O-Oleuropeoylsucrose	$C_{22}H_{36}O_{13}$	43, 147, 299, 327, 475
125	514.265	-	-	-	-	-	
126	518.285	-	-	-	-	-	
127	524.274	524.2731	2	$[M-H]^-$	Isodesmosine	$C_{24}H_{40}N_5O_8$	45, 132, 490
128	533.291	533.2885	5	$[M-H]^-$	LPG (20:3)	$C_{26}H_{47}O_9P$	97, 153, 227, 245, 305, 533
129	535.214	535.2185	8	$[M-H]^-$	Quassimarin	$C_{27}H_{36}O_{11}$	59, 115, 287, 363, 447
130	537.218	-	-	-	-	-	
131	546.312	-	-	-	-	-	
132	548.334	-	-	-	-	-	
133	552.273	552.2715	3	$[M-H]^-$	Vignatic acid A	$C_{30}H_{39}N_3O_7$	57, 85, 331, 392, 438
134	553.182	-	-	-	-	-	
135	568.218	568.2188	1	$[M-H]^-$	Aklavin	$C_{30}H_{35}NO_{10}$	59, 129, 281, 377, 411, 568
136	574.320	-	-	-	-	-	
137	576.347	-	-	-	-	-	
138	582.268	582.2722	7	$[M-H]^-$	Dihydroegotamine	$C_{33}H_{37}N_5O_5$	42, 103, 209, 358, 450, 580
139	587.353	587.3589	10	$[M-H]^-$	25-Hydroxyvitamin D2-25-glucuronide	$C_{34}H_{52}O_8$	59, 131, 311, 411, 481
140	589.357	589.3615	8	$[M-H]^-$	Benextramine	$C_{32}H_{54}N_4O_2S_2$	59, 120, 248, 347, 453
141	590.276	-	-	-	-	-	
142	595.201	-	-	-	-	-	

No.	Measured *m/z*	Calculated *m/z*	Error |ppm|	Assignment			Structurally specific CID ions (*m/z*) a)
				Ion form	Compound	Molecular formula	
143	603.367	603.3667	0	$[M-H]^-$	PA(28:2)	$C_{31}H_{57}O_9P$	79, 171, 295, 325, 431, 449
144	605.384	-	-	-	-	-	
145	613.353	-	-	-	-	-	
146	615.389	615.3902	2	$[M-H]^-$	13-O-Tetradecanoylphorbol 12-acetate	$C_{36}H_{56}O_8$	59, 127, 209, 405, 547, 615
147	617.403	-	-	-	-	-	
148	619.417	619.4215	7	$[M-H]^-$	Glucoside Rh4	$C_{36}H_{60}O_8$	59, 499, 603
149	622.371	622.3726	3	$[M-H]^-$	PS(24:0)	$C_{30}H_{58}NO_{10}P$	79, 97, 153, 199, 353, 535, 622
150	643.403	-	-	-	-	-	
151	645.425	-	-	-	-	-	
152	647.435	-	-	-	-	-	
153	649.429	-	-	-	-	-	
154	651.443	651.4395	5	$[M-H]^-$	PA (O-34:5)	$C_{37}H_{65}O_7P$	79, 97, 171, 275, 393
155	659.492	-	-	-	-	-	
156	671.459	671.4657	10	$[M-H]^-$	PA(34:2)	$C_{37}H_{69}O_8P$	79, 97, 209, 307, 671
157	673.483	673.4814	2	$[M-H]^-$	PA(34:1)	$C_{37}H_{71}O_8P$	79, 237, 255, 279, 673
158	693.447	693.4501	4	$[M-H]^-$	PA(36:5)	$C_{39}H_{67}O_8P$	97, 283, 313 581, 651
159	698.507	698.5130	9	$[M-H]^-$	PE(P-34:2)	$C_{39}H_{74}NO_7P$	79, 93, 140, 253, 389, 417
160	699.509	-	-	-	-	-	
161	700.529	700.5287	0	$[M-H]^-$	PE(P-34:1)	$C_{39}H_{76}NO_7P$	79, 93, 255, 391, 545
162	701.489	-	-	-	-	-	
163	702.533	-	-	-	-	-	
164	714.503	714.5079	7	$[M-H]^-$	PE(34:2)	$C_{39}H_{74}NO_8P$	153, 227, 406, 504
165	716.517	716.5236	9	$[M-H]^-$	PE(34:1)	$C_{39}H_{76}NO_8P$	153, 255, 434, 478, 717
166	719.471	719.4657	7	$[M-H]^-$	PA(38:6)	$C_{41}H_{69}O_8P$	79, 153, 255, 409, 719
167	721.476	721.4814	7	$[M-H]^-$	PA(38:5)	$C_{41}H_{71}O_8P$	79, 153, 255, 391, 721
168	726.549	726.5443	6	$[M-H]^-$	PE(P-36:2)	$C_{41}H_{78}NO_7P$	79, 571

No.	Measured *m/z*	Calculated *m/z*	Error |ppm|	Assignment			Structurally specific CID ions (*m/z*) [a)]
				Ion form	Compound	Molecular formula	
169	728.565	728.5600	0	$[M-H]^-$	PE(P-36:1)	$C_{41}H_{80}NO_7P$	79, 265, 729 79, 140, 265, 283, 419, 729
170	731.517	731.5233	9	$[M-H]^-$	PG (O-34:2)	$C_{40}H_{77}O_9P$	79, 93, 159, 209, 377, 469, 657
171	736.488	736.4923	6	$[M-H]^-$	PE(P-36:5)	$C_{41}H_{72}NO_8P$	63,79, 239, 445, 573
172	738.495	-	-	-	-	-	
173	742.534	742.5392	7	$[M-H]^-$	PE(36:2)	$C_{41}H_{78}NO_8P$	196, 281, 460, 478, 743
174	744.551	744.5549	0	$[M-H]^-$	PE(36:1)	$C_{41}H_{80}NO_8P$	153, 339, 536
175	745.482	745.4814	1	$[M-H]^-$	PA(40:7)	$C_{43}H_{71}O_8P$	153, 281, 327, 435, 481, 745
176	746.535	746.5342	1	$[M-H]^-$	PS (O-34:1)	$C_{40}H_{78}NO_9P$	79, 97, 153, 281, 395, 660
177	747.526	-	-	-	-	-	
178	748.545	748.5498	6	$[M-H]^-$	PS (O-34:0)	$C_{40}H_{80}NO_9P$	79, 283, 662
179	750.511	750.5079	4	$[M-H]^-$	PC(34:5)	$C_{42}H_{74}NO_8P$	59, 127, 227, 301, 453, 647
180	758.523	-	-	-	-	-	
181	762.513	762.5079	7	$[M-H]^-$	PE(38:6)	$C_{43}H_{74}NO_8P$	275, 307, 763 153, 275, 307, 486, 763
182	764.540	-	-	-	-	-	
183	766.542	766.5392	0	$[M-H]^-$	PE(38:4)	$C_{43}H_{78}NO_8P$	259, 283, 303, 462, 480, 482, 500, 767
184	770.548	-	-	-	-	-	
185	772.555	772.5498	7	$[M-H]^-$	PS (O-36:2)	$C_{42}H_{80}NO_9P$	79, 93, 157, 377, 395, 686, 773
186	773.547	-	-	-	-	-	
187	774.551	774.5443	9	$[M-H]^-$	PE(P-40:6)	$C_{45}H_{78}NO_7P$	83, 122, 265, 329, 465, 620
188	775.543	775.5495	8	$[M-H]^-$	PG(36:1)	$C_{42}H_{81}O_{10}P$	79, 281, 417, 702 79, 281, 433, 590, 684, 758

No.	Measured *m/z*	Calculated *m/z*	Error |ppm|	Assignment			Structurally specific CID ions (*m/z*) [a]
				Ion form	Compound	Molecular formula	
189	776.526	776.5236	3	$[M-H]^-$	PC(36:6)	$C_{44}H_{76}NO_8P$	79, 183, 227, 327, 581, 673
190	778.563	-	-	-	-	-	
191	786.487	786.4927	7	$[M-H]^-$	PC(34:5)	$C_{42}H_{74}NO_8P$	59, 227, 301, 453
192	788.528	788.5236	6	$[M-H]^-$	PE (40:7)	$C_{45}H_{76}NO_8P$	79, 97, 153, 283, 327, 478, 524
193	790.558	790.5604	0	$[M-H]^-$	PS(36:0)	$C_{42}H_{82}NO_{10}P$	79, 686
194	792.552	792.5549	4	$[M-H]^-$	PE(40:5)	$C_{45}H_{80}NO_8P$	153, 283, 329, 462, 480, 508, 526
195	804.543	804.5479	6	$[M-H]^-$	LacCer(d30:1)	$C_{42}H_{79}NO_{13}$	59, 137, 224, 402, 762, 745
196	807.545	-	-	-	-	-	
197	808.543	808.5498	8	$[M-H]^-$	PE (40:5-OH)	$C_{45}H_{80}NO_9P$	153, 196, 309, 488, 516, 809
198	809.562	809.5702	10	$[M-H]^-$	PG (O-40:5)	$C_{46}H_{83}O_9P$	79, 153, 209, 301, 433, 451, 525, 736
199	810.533	810.5291	5	$[M-H]^-$	PS(38:4)	$C_{44}H_{78}NO_{10}P$	153, 279, 415, 723, 811
200	814.517	-	-	-	-	-	
201	816.565	-	-	-	-	-	
202	818.579	818.5705	10	$[M-H]^-$	PE (42:6)	$C_{47}H_{82}NO_8P$	97, 122, 283, 327, 506, 819
203	821.542	821.5338	10	$[M-H]^-$	PG (40:6)	$C_{46}H_{79}O_{10}P$	79, 153, 245, 327, 437, 493, 555, 747
204	822.558	822.5655	9	$[M-H]^-$	PS (O-40:5)	$C_{46}H_{82}NO_9P$	79, 97, 153, 257, 301, 451, 736, 823
205	828.533	828.5396	8	$[M-H]^-$	PS (38:3-OH)	$C_{44}H_{80}NO_{11}P$	153, 293, 311, 447, 742, 829
206	832.544	832.5498	7	$[M-H]^-$	PE (42:7-OH)	$C_{47}H_{80}NO_9P$	153, 196, 331, 500, 528, 833
207	833.561	833.5549	7	$[M-H]^-$	PE (38:2-2OH)	$C_{44}H_{83}O_{12}P$	153, 171, 313, 445, 519, 541
208	834.550	-	-	-	-	-	
209	835.585	-	-	-	-	-	

No.	Measured *m/z*	Calculated *m/z*	Error |ppm|	Assignment			Structurally specific CID ions (*m/z*) [a)]
				Ion form	Compound	Molecular formula	
210	836.538	836.5447	8	$[M-H]^-$	PS (40:5)	$C_{46}H_{80}NO_{10}P$	79, 97, 153, 287, 331, 767, 750
211	846.501	846.4927	10	$[M-H]^-$	PS (40:8-OH)	$C_{46}H_{74}NO_{11}P$	153, 303, 439, 473, 759, 846
212	848.543	848.5447	2	$[M-H]^-$	PE (42:7-2OH)	$C_{47}H_{80}NO_{10}P$	153, 196, 337, 510, 534, 849
213	856.553	-	-	-	-	-	
214	857.562	857.5549	8	$[M-H]^-$	PG (42:4-2OH)	$C_{46}H_{83}O_{12}P$	153, 303, 337, 473, 519, 565, 858
215	860.641	860.6386	3	$[M-H]^-$	PE (42:1-2OH)	$C_{47}H_{92}NO_{10}P$	153, 492, 861
216	862.603	862.5967	7	$[M-H]^-$	PE (44:6-OH)	$C_{49}H_{86}NO_9P$	153, 196, 343, 518, 540, 863
217	863.637	-	-	-	-	-	
218	876.570	876.5760	7	$[M-H]^-$	PE (44:7-2OH)	$C_{49}H_{84}NO_{10}P$	153, 196, 337, 516, 556
219	878.486	878.4825	4	$[M-H]^-$	PE (40:8-3OH)	$C_{46}H_{74}NO_{13}P$	153, 305, 349, 441, 485, 791, 878
220	881.543	-	-	-	-	-	
221	883.569	-	-	-	-	-	
222	885.587	-	-	-	-	-	
223	888.679	-	-	-	-	-	
224	894.519	-	-	-	-	-	
225	900.502	900.4962	6	$[M-H]^-$	beta1-Tomatidine	$C_{45}H_{75}NO_{17}$	43, 179, 323, 414, 576, 810, 868
226	904.664	-	-	-	-	-	
227	909.556	909.5499	7	$[M-H]^-$	PI(40:6)	$C_{49}H_{83}O_{13}P$	79, 179, 241, 327, 479, 639, 729
228	939.564	939.5604	4	$[M-H]^-$	PG (40:6-OH)	$C_{50}H_{85}O_{14}P$	293, 429, 483, 645, 663, 940
229	1023.555	-	-	-	-	-	
230	1069.512	1069.5060	6	$[M-H]^-$	PG (44:10-2OH)	$C_{53}H_{84}O_{18}P_2$	79, 137, 285, 395, 467, 719, 979
231	1071.506	-	-	-	-	-	
232	1084.501	-	-	-	-	-	

No.	Measured *m/z*	Calculated *m/z*	Error |ppm|	Assignment			Structurally specific CID ions (*m/z*) [a)]
				Ion form	Compound	Molecular formula	
233	1086.489	1086.4863	3	$[M-H]^-$	CDP-DG(42:11-O)	$C_{54}H_{79}N_3O_{16}P_2$	59, 159, 384, 442, 558, 768, 843, 1028
234	1097.464	-	-	-	-	-	
235	1110.552	1110.5438	7	$[M-H]^-$	CDP-DG(42:7-2OH)	$C_{54}H_{87}N_3O_{17}P_2$	71, 159, 291, 384, 559, 720, 851, 1093
236	1112.437	1112.4315	5	$[M-H]^-$	(13Z,16Z)-Tetracosa-13,16-dienoyl-CoA	$C_{45}H_{78}N_7O_{17}P_3S$	79, 328, 344, 408, 488, 635,716, 776
237	1114.451	1114.4472	3	$[M-H]^-$	Nervonyl CoA	$C_{45}H_{80}N_7O_{17}P_3S$	79, 143, 159, 344, 424, 488, 716
238	1116.463	1116.4628	0	$[M-H]^-$	Methyltricosanoyl-CoA	$C_{45}H_{82}N_7O_{17}P_3S$	79, 143, 159, 408, 488, 635, 716, 776
239	1140.398	1140.3900	7	$[M-H]^-$	Deoxycholoyl-CoA	$C_{45}H_{74}N_7O_{19}P_3S$	79, 159, 179, 373, 488, 713, 793, 1122
240	1156.394	1156.3849	8	$[M-H]^-$	Choloyl-CoA	$C_{45}H_{74}N_7O_{20}P_3S$	79, 134, 159, 389, 488, 729, 1138
241	1158.388	-	-	-	-	-	
242	1182.388	-	-	-	-	-	
243	1184.443	-	-	-	-	-	
244	1218.291	-	-	-	-	-	
245	1424.803	-	-	-	-	-	
246	1470.548	-	-	-	-	-	
247	1494.456	-	-	-	-	-	
248	1495.973	1495.9650	5	$[M-H]^-$	CL(76:12)	$C_{85}H_{142}O_{17}P_2$	253, 329, 389, 465, 591, 747
249	1499.492	-	-	-	-	-	
250	1516.134	1516.1215	8	$[M-H]^-$	CL(76:2)	$C_{85}H_{162}O_{17}P_2$	255, 297, 353, 489, 638, 758
251	1541.962	1541.9493	8	$[M-H]^-$	CL(80:17)	$C_{89}H_{140}O_{17}P_2$	253, 327, 463, 615, 770
252	1567.963	1567.9650	1	$[M-H]^-$	CL(82:18)	$C_{91}H_{142}O_{17}P_2$	255, 327, 463, 628, 783
253	1587.895	-	-	-	-	-	

a) Structurally specific CID ions of extracted compounds were detected by LC-MS/MS and/or MALD-TOF/TOF MS/MS using CID.
Red fragment ions were detected by LC-MS/MS, and blue fragment ions were detected by MALD-TOF/TOF MS/MS.

Reference

1. K. A. Nelson, G. J. Daniels, J. W. Fournie and M. J. Hemmer, *J Biomol Tech*, 2013, **24**, 119-127.
2. A. Dannhorn, E. Kazanc, S. Ling, C. Nikula, E. Karali, M. P. Serra, J. L. Vorng, P. Inglese, G. Maglennon, G. Hamm, J. Swales, N. Strittmatter, S. T. Barry, O. J. Sansom, G. Poulogiannis, J. Bunch, R. J. Goodwin and Z. Takats, *Anal. Chem.*, 2020, **92**, 11080-11088.
3. X. Wang, J. Han, J. Yang, J. Pan and C. H. Borchers, *Chem Sci*, 2015, **6**, 729-738.
4. K.-H. Nam, D. Y. Kim, H. J. Kim, I.-S. Pack, H. J. Kim, Y. S. Chung, S. Y. Kim and C.-G. Kim, *Applied Biological Chemistry*, 2019, **62**, 15.
5. A. Ly, A. Buck, B. Balluff, N. Sun, K. Gorzolka, A. Feuchtinger, K.-P. Janssen, P. J. K. Kuppen, C. J. H. van de Velde, G. Weirich, F. Erlmeier, R. Langer, M. Aubele, H. Zitzelsberger, L. McDonnell, M. Aichler and A. Walch, *Nat. Protoc.*, 2016, **11**, 1428-1443.